



HAL
open science

Survey on signal processing for GNSS under ionospheric scintillation: Detection, monitoring, and mitigation

Jordi Vilà Valls, Nicola Linty, Pau Closas, Fabio Dovis, James T. Curran

► To cite this version:

Jordi Vilà Valls, Nicola Linty, Pau Closas, Fabio Dovis, James T. Curran. Survey on signal processing for GNSS under ionospheric scintillation: Detection, monitoring, and mitigation. *Navigation*, 2020, 67 (3), pp.511-536. 10.1002/navi.379 . hal-03033036

HAL Id: hal-03033036

<https://hal.science/hal-03033036>

Submitted on 1 Dec 2020

HAL is a multi-disciplinary open access archive for the deposit and dissemination of scientific research documents, whether they are published or not. The documents may come from teaching and research institutions in France or abroad, or from public or private research centers.

L'archive ouverte pluridisciplinaire **HAL**, est destinée au dépôt et à la diffusion de documents scientifiques de niveau recherche, publiés ou non, émanant des établissements d'enseignement et de recherche français ou étrangers, des laboratoires publics ou privés.



Open Archive Toulouse Archive Ouverte (OATAO)

OATAO is an open access repository that collects the work of some Toulouse researchers and makes it freely available over the web where possible.

This is an author's version published in: <https://oatao.univ-toulouse.fr/26949>

Official URL : <https://doi.org/10.1002/navi.379>


To cite this version :

Vilà Valls, Jordi and Linty, Nicola and Closas, Pau and Dovis, Fabio and Curran, James T. Survey on signal processing for GNSS under ionospheric scintillation: Detection, monitoring, and mitigation. (2020) Journal of the Institute of Navigation, 67 (3). 511-536. ISSN 0028-1522

Any correspondence concerning this service should be sent to the repository administrator:

tech-oatao@listes-diff.inp-toulouse.fr

Survey on signal processing for GNSS under ionospheric scintillation: Detection, monitoring, and mitigation

Jordi Vilà-Valls¹  | Nicola Linty²  | Pau Closas³  | Fabio Dovis⁴ | James T. Curran⁵

¹ ISAE-SUPAERO, University of Toulouse, Toulouse, France

² Finnish Geospatial Research Institute (FGI-NLS), Helsinki, Finland

³ Electrical and Computer Engineering Department, Northeastern University, Boston, MA, USA

⁴ Department of Electronics and Telecommunications (DET), Politecnico di Torino, Torino, Italy

⁵ European Commission Joint Research Centre Ispra Sector, Institute for the Protection and Security of the Citizen, Adamstown, Ballinacorney, Cork T12F24N, Ireland

Correspondence

Jordi Vilà-Valls, ISAE-SUPAERO, University of Toulouse, Toulouse, France.
Email: jordi.vila-valls@isae-supaeero.fr

Funding information

National Science Foundation, Grant/Award Numbers: CNS-1815349, ECCS-1845833; DGA/AID, Grant/Award Number: 2019.65.0068.00.470.75 01

Abstract

Ionospheric scintillation is the physical phenomena affecting radio waves coming from the space through the ionosphere. Such disturbance is caused by ionospheric electron-density irregularities and is a major threat in Global Navigation Satellite Systems (GNSS). From a signal-processing perspective, scintillation is one of the most challenging propagation scenarios, particularly affecting high-precision GNSS receivers and safety critical applications where accuracy, availability, continuity, and integrity are mandatory. Under scintillation, GNSS signals are affected by amplitude and phase variations, which mainly compromise the synchronization stage of the receiver. To counteract these effects, one must resort to advanced signal-processing techniques such as adaptive/robust methods, machine learning, or parameter estimation. This contribution reviews the signal-processing landscape in GNSS receivers, with emphasis on different detection, monitoring, and mitigation problems. New results using real data are provided to support the discussion. To conclude, future perspectives of interest to the GNSS community are discussed.

KEYWORDS

carrier synchronization, detection, GNSS, ionospheric scintillation, mitigation, monitoring, robust tracking

1 | INTRODUCTION

Precise and reliable positioning is nowadays of paramount importance in several mass-market civil, industrial and transport applications, safety-critical receivers, and a plethora of engineering fields. In general, GNSS is the positioning technology of choice, but these systems were originally designed to operate under clear skies and its performance clearly degrades under non-nominal conditions (Dardari, Closas, & Djurić, 2015; Dardari, Falletti, & Luise, 2011; Fernández-Prades, Lo Presti, & Falletti, 2011). Therefore, the main drawback on the use of GNSS rises in challenging harsh propagation scenarios naturally

impaired by multipath, shadowing, high dynamics, strong fading, or ionospheric scintillation (Seco-Granados, Lopez-Salcedo, Jiménez-Baños, & López-Risueño, 2012). In the last decade, the mitigation of such vulnerabilities has been the main driver on advanced receiver design to provide position accuracy, reliability, and integrity (Amin, Closas, Broumandan, & Volakis, 2016). From a signal-processing perspective (Closas, Luise, Avila-Rodriguez, Hegarty, & Lee, 2017), ionospheric scintillation detection, monitoring, and mitigation are certainly some of the more challenging and appealing GNSS scenarios. Because ionospheric scintillation is not related to the local environment, as in the case of multipath or shadowing, it can degrade

receiver performance even under ideal open-sky conditions (Vilà-Valls, Closas, Fernández-Prades, & Curran, 2018). As it will be later explained in detail, ionospheric scintillation may induce fast phase variations (i.e., phase scintillation) and deep amplitude fades (i.e., amplitude scintillation), effects which are frequency and latitude dependent. Both need to be considered in the design of scintillation resilient receivers.

Early GNSS receivers operated only on the principle of code-delay ranging, as do many low-cost, low-power mass-market receivers. Because the principal impact of ionospheric scintillation is on the carrier-phase estimation, such receivers are relatively insensitive to it (i.e., notice that this refers to the stronger impact on carrier tracking rather than code tracking, but both amplitude and phase scintillation must be taken into account). This, and the fact that severe scintillation only appears in equatorial and high-latitude regions for short periods of time, is the main reason why counteracting such propagation effects has attracted rather little attention among the signal-processing community, and thus compared to other fields of study, there are few contributions in the literature. However, much of the improvement in positioning accuracy provided by modern receivers is due to their exploitation of carrier-phase measurements. As a result, many modern receivers, and most notably high-precision receivers, are extremely sensitive to ionospheric scintillation (Banville & Langley, 2013; Banville, Langley, Saito, & Yoshihara, 2010; Jacobsen & Dähnn, 2014; Linty, Minetto, DAVIS, & Spogli, 2018; Prikryl, Jayachandran, Mushini, & Richardson, 2014).

Under open-sky conditions, the primary contributors to positioning inaccuracy for a stand-alone GNSS receiver are satellite clock and ephemeris errors and unmodeled atmospheric effects. Orbit and clock models, broadcast by the satellite, are typically accurate to the meter level (Warren & Raquet, 2003). Ephemeris and clock errors will be common to two receivers that are simultaneously observing a set of satellites, and so relative positioning approaches, known as differential positioning (or Differential GNSS, DGNSS), can significantly reduce these factors. Also, by using a wide network of reference stations, precise clock and orbit models can be produced, in which these errors are significantly smaller, typically of the order of a few centimeters. Both the troposphere and the ionosphere contribute to the atmospheric effects, being of the order of 1-10 meters and 5-25 meters, respectively. In both cases, these errors are reasonably well correlated over space and so can be eliminated in a DGNSS receiver. For the stand-alone user, many models exist for the correction of tropospheric errors, which are generally accurate to some centimeters, or tens of centimeters. The ionosphere is somewhat more challenging, being less spatially and temporally

correlated, and subject to more sporadic disturbances, correction models generally leave of the order of 10 meters of uncorrected error. However, the delay observed on signals at different frequencies is related by its refractive index and is proportional inverse square of the center frequency of each signal. When the ionosphere varies smoothly, this relationship holds, and a receiver can track this varying ionospheric delay and make appropriate corrections to the observed range.

With all of these factors considered, the resultant positioning error is driven primarily by the ranging accuracy of the receiver. This can be significantly reduced by either of two means: carrier smoothing of the pseudorange estimate or carrier-phase-based positioning. Carrier-phase-based positioning, being either differential, such as real-time-kinematic (RTK), or stand-alone, such as precise-point-positioning (PPP), provides a tremendous improvement in accuracy and can result in positioning errors of less than one centimeter. Achieving this requires high accuracy carrier-phase tracking, which can be very challenging under ionospheric scintillation conditions.

The impact of ionospheric scintillation on GNSS signals is handled by current receiver technology in a number of different manners, depending on the particular application. For general purpose navigation receivers, the approach is generally to provide robustness, wherein the receiver strives to tolerate the signal fluctuations and continue to derive positioning measurements from the signal. For high-integrity applications, however, identification of potential scintillation episodes is more important, and the receiver may strive to detect and reject the corresponding measurements. Finally, for space weather monitoring, there has been a trend towards vector receivers and beyond this to open-loop processing, wherein the static receiver fully exploits knowledge of the location, clock, and satellite orbital parameters to reduce the overall tracking uncertainty. In this situation, the primary goal of a receiver is to extract information (typically off-line) about the scintillation process rather than achieving a robust position solution.

It is worth mentioning that in recent years there is an increasing interest on the topic of scintillation detection, monitoring, and mitigation in both research and industry. For instance, two major GNSS receiver manufacturers have their own ionospheric scintillation monitoring receiver, namely, the NovAtel's GPStation-6 <https://novatel.com/support/previous-generation-products-drop-down/previous-generationproducts/gpstation-6-receiver> and Septentrio's PolaRx5S <https://www.septentrio.com/en/products/gnss-receivers/reference-receivers/polarx5s>. On the academic side, some of the latest research activities funded by the European Commission (EC) and the European Space Agency (ESA)

are projects such as CIGALA (Concept for Ionospheric Scintillation Mitigation for Professional GNSS in Latin America, <http://www.gsa.europa.eu/conceptionospheric-scintillation-mitigation-professional-gnss-latin-america>), CALIBRA (Countering GNSS high Accuracy applications Llimitation due to ionospheric disturbance in BRAzil), <http://www.calibra-ionosphere.net/calibra/index.aspx>), MImOSA (Monitoring Ionosphere Over South America to support high-precision applications; Cesaroni et al., 2015), TRANSMIT (Training Research and Applications Network to Support the Mitigation of Ionospheric Threats, <http://www.nottingham.ac.uk/transmit/index.aspx>) or MONITOR (MONitoring of the Ionosphere by innovative Techniques, coordinated Observations and Resources; Prieto Cerdeira & Béniguel, 2011). It is a fact that the fundamental background to these activities; to solving the ionospheric scintillation detection, monitoring, and mitigation problems; and providing a strong theoretical understanding is signal processing.

This paper provides a survey on the design of GNSS receivers that *i*) are able to detect ionospheric scintillation events, *ii*) reliably monitor the ionosphere, and/or *iii*) are resilient to ionospheric scintillation conditions. The focus is on the statistical signal processing and learning aspects of those receivers.

2 | BACKGROUND ON GNSS AND IONOSPHERIC SCINTILLATION

2.1 | GNSS signal modeling

A GNSS satellite transmits a low-rate navigation message modulated by a unique spreading sequence or code. A generic baseband analytic representation of such signal is

$$s_i(t) = \sqrt{2P(t)}d(t - \tau_i(t))c_i(t - \tau_i(t))e^{j\theta_i(t)}, \quad (1)$$

where $P(t)$, $d(t)$, and $c_i(t)$ stand for the received power, the navigation message, and the spreading code of the i -th satellite, respectively. The synchronization parameters are the, $\tau_i(t)$, and the carrier phase, $\theta_i(t)$. The latter can be formulated as $\theta_i(t) = 2\pi f_{d,i}(t) + \theta_{e,i}(t)$, where $f_{d,i}(t)$ is the carrier Doppler frequency shift and $\theta_{e,i}(t)$ a carrier-phase component including other phase impairments (Kaplan, 2006). The received signal is therefore the linear combination of the signals transmitted by M visible satellites plus noise:

$$y(t) = \sum_{i=1}^M s_i(t) + w(t), \quad (2)$$

where $w(t)$ is a zero-mean noise process usually modelled as white and Gaussian with power spectral density N_0 . After downconversion and filtering with bandwidth B , the signal is sampled at a sampling rate of $f_s = 1/T_s$ such that the digital baseband signal is $y[n] = y(nT_s)$ with n being the discrete-time index. The signal is then processed in order to determine the number of available satellites, as well as to compute rough estimates of the time-delay and Doppler-shift for each detected satellite in a process typically referred to as acquisition. Afterwards, such parameters are fine-tracked such that accurate estimates are available for later PVT computation.

In both acquisition and tracking stages, the sampled signal is correlated with a locally generated replica and then accumulated over an integration period T_I . Dropping the satellite index i for simplicity, the samples at the output of the correlators are Spilker (1996) usually expressed as

$$y_k = A_k d_k R(\Delta\tau_k) \frac{\sin(\pi\Delta f_{d,k}T_I)}{\pi\Delta f_{d,k}T_I} e^{j(2\pi\Delta f_{d,k}T_I + \Delta\theta_k)} + w_k,$$

where k stands for the discrete-time sample index after correlating with integration period T_I , that is $t_k = kT_I$. A_k is the signal amplitude at the output of the correlators, $d_k \in \{-1, 1\}$ is the data bit polarity, $R(\cdot)$ is the code autocorrelation function, and $\{\Delta\tau_k, \Delta f_{d,k}, \Delta\theta_k\}$ are, respectively, the code delay, Doppler shift, and carrier-phase errors that the tracking loops aim at minimizing. The noise at the output of the correlators is considered additive complex Gaussian with variance $\sigma_{w,k}^2$, that is, $w_k \sim \mathcal{CN}(0, \sigma_{w,k}^2)$. If we assume perfect timing synchronization and data wipe-off, a simplified model for the samples at the input of the carrier-phase tracking stage can be written as $y_k = A_k e^{j\theta_k} + w_k \in \mathbb{C}$, or equivalently in terms of its in-phase and quadrature components

$$\begin{pmatrix} y_{I,k} \\ y_{Q,k} \end{pmatrix} = A_k \begin{pmatrix} \cos(\theta_k) \\ \sin(\theta_k) \end{pmatrix} + \begin{pmatrix} w_{I,k} \\ w_{Q,k} \end{pmatrix}, \quad (3)$$

such that $y_k = y_{I,k} + iy_{Q,k}$ and $w_k = w_{I,k} + iw_{Q,k}$, with covariance matrix $\mathbf{R}_k = \sigma_{w,k}^2/2 \mathbf{I}_2$. In this context, a carrier-tracking method is in charge of estimating over time the carrier phase θ_k in Equation (3). In its simplest modeling, that is without ionospheric scintillation contribution, such phase is primarily composed of terms due to the relative dynamics of the receiver and the satellite $\theta_k \doteq \theta_{d,k}$. An expression can be obtained using a fourth-order Taylor approximation of the time-varying phase evolution as

$$\theta_{d,k} = \theta_0 + 2\pi(f_{d,k}kT_s + \underbrace{f_{r,k}k^2T_s^2/2 + f_{j,k}k^3T_s^3/6}_{\text{Doppler dynamics}}), \quad (4)$$

where θ_0 (rad) is a random constant phase value, $f_{d,k}$ (Hz) the carrier Doppler frequency shift, $f_{r,k}$ (Hz/s) the Doppler frequency rate, and $f_{j,k}$ (Hz/s²) the Doppler acceleration. Notice that the phase can be expressed recursively as

$$\begin{pmatrix} \theta_{d,k} \\ f_{d,k} \\ f_{r,k} \\ f_{j,k} \end{pmatrix} = \begin{pmatrix} 1 & 2\pi T_I & \pi T_I^2 & \pi T_I^3/3 \\ 0 & 1 & T_I & T_I^2/2 \\ 0 & 0 & 1 & T_I \\ 0 & 0 & 0 & 1 \end{pmatrix} \begin{pmatrix} \theta_{d,k-1} \\ f_{d,k-1} \\ f_{r,k-1} \\ f_{j,k-1} \end{pmatrix} \quad (5)$$

which is very convenient for state-space formulations of the tracking problem (Vilà-Valls, Closas, Fernández-Prades, & Curran, 2018). Lower order dynamics can be considered if only the first-order terms are kept, for instance $\theta_{d,k-1}$ and $f_{d,k-1}$.

Notice that most works dealing with ionospheric scintillation consider only the impact of it on the received carrier phase $\theta_i(t)$, that is, how both amplitude and phase scintillation affect the performance of carrier-phase estimation techniques. The impact on the time-delay $\tau_i(t)$ is typically neglected as the variability of scintillation-induced phase does not compare to the actual variability of code-phase tracking loops. More precisely, the correlation outputs used by delay-lock loops (DLL) are sensitive to residual errors on 1) the carrier-phase (Doppler) frequency via a the $\text{sinc}(\pi\Delta f_{d,k}T_I)$ function appearing in the equation for y_k ; and 2) to the average code-phase alignment over the correlation period, via the code autocorrelation function $R(\Delta\tau_k)$. Since the width of the code correlation is of the order of some tens or hundreds of meters, depending on the GNSS signal, short-term (or even long-term) variations in the ionosphere delay coefficient will not have an appreciable impact on its magnitude since its variability is much less. On the other side, ionospheric scintillation impacts also the amplitude of the received signal, as discussed in the next subsection, but again this will always have more impact on the carrier estimation than on the code-tracking stage.

2.2 | Ionospheric scintillation modeling

The ionosphere is a region of the upper atmosphere, from about 85 km to 600 km altitude, that is ionized by solar radiation. It constitutes a plasmatic media that causes a group delay of the modulation and a phase advance on the electromagnetic waves that propagate through it. Ionospheric scintillation is created by diffraction when the transmitted propagating electromagnetic waves encounter a medium made of irregular structures with variable refraction indices, such as the plasma bubbles with a weak ionization level that appear frequently after sunset in the lower part of the ionosphere (Humphreys, Psiaki, & Kintner, 2010;

Kintner et al., 2009). The recombination of waves after propagation can be constructive or destructive, and the resulting signal at the receiver antenna may present rapid variations of phase and amplitude. It is important to notice that those amplitude fades and phase changes happen in a simultaneous and random manner, but there exists a correlation between both disturbances, the so-called canonical fades. That is, the largest amplitude fades are regularly associated with very rapid phase inversions in the received signal (Humphreys, Psiaki, & Kintner, 2010; Kintner et al., 2009), which is a very challenging carrier-tracking scenario.

A lot of effort has been put in the past two decades to characterize the ionospheric scintillation, mainly targeted to obtain effective synthetic models to assess GNSS receivers' performance via simulation. At the time of writing, this is a list of popular ionospheric scintillation models:

- The WideBand MODel (WBMOD) provides the global distribution and synoptic behavior of the electron-density irregularities that cause scintillation and a propagation model that calculates the effects these irregularities will have on a given system (Secan, Bussey, & Fremouw, 1997).
- Phase-screen scintillation models are sometimes used to provide a relatively simple physical model that is applicable in equatorial scintillation (Beach, 1998; Psiaki et al., 2007)
- Global Ionospheric Scintillation Model (GISM, 2013), based on a phase-screen technique driven by the NeQuick electron-density climatological model (Di Giovanni & Radicella, 1990).
- Cornell Scintillation Model (CSM) (Humphreys, Psiaki, Hinks, O'Hanlon, & Kintner, 2009, 2010), based on a statistical model and the proper shaping of the spectrum of the entire complex scintillation signal. A Matlab toolbox is available at <https://gps.ece.cornell.edu/tools.php>.
- Recently, a new scintillation simulation method has been presented in Jiao, Xu, Rino, Morton, and Carrano (2018); Jiao, Rino, and Morton (2018); and Rino et al. (2018). The main advantage is that it allows generation of scintillation for dynamic platforms. A Matlab toolbox is available at <https://github.com/cu-sense-lab/gnss-scintillation-simulator>.

The behavior of scintillation on GNSS signals can be modeled as a multiplicative channel, resulting in a commonly adopted model. In that case, Equation (2) is modified as

$$y(t) = \sum_{i=1}^M \xi_{s,i}(t)s_i(t) + w(t), \quad (6)$$

where, if we again omit the dependence on each satellite's propagation path, the disturbance caused by ionospheric scintillation is defined as

$$\xi_s(t) = \rho_s(t)e^{j\theta_s(t)}, \quad (7)$$

with $\rho_s(t)$ and $\theta_s(t)$ being the corresponding envelope and phase components. The severity of the scintillation is traditionally quantified by two indices: an *amplitude-scintillation index*, S_4 ; and a *phase-scintillation index*, σ_ϕ . The indices are computed on a per-signal basis and indicate average intensity of the signal variations over the preceding minute. They have been used for some decades, and as a result, there exist rich databases of historical data for a wide range of observation points.

The S_4 amplitude-scintillation strength is defined as follows and is usually considered within three main regions (Humphreys et al., 2009):

$$S_4 = \sqrt{\frac{\langle \rho_s^4 \rangle - \langle \rho_s^2 \rangle^2}{\langle \rho_s^2 \rangle^2}}, \begin{cases} S_4 \leq 0.4 \text{ (weak)} \\ 0.4 < S_4 \leq 0.6 \text{ (mod.)} \\ 0.6 < S_4 \text{ (sev.)} \end{cases} \quad (8)$$

$\langle \cdot \rangle$ being the time average operator. Equivalently, the phase-scintillation index σ_ϕ is defined as

$$\sigma_\phi = \sqrt{\langle \theta_{s,d}^2 \rangle - \langle \theta_{s,d} \rangle^2}, \quad (9)$$

$$\begin{cases} \sigma_\phi \leq 0.25 \text{ rad (weak)} \\ 0.25 \text{ rad} < \sigma_\phi \leq 0.5 \text{ rad (mod.)} \\ 0.5 \text{ rad} < \sigma_\phi \text{ (sev.)} \end{cases} \quad (9)$$

where $\theta_{s,d}$ is the phase term θ_s after detrending through a sixth-order Butterworth high-pass filter, i.e., standard deviation of the detrended phase measurement over the one-minute interval.

Scintillation affects the signal before it arrives at the receiver. After downconverting and sampling, the signal is correlated with a local code, as explained in the previous subsection. The simplified signal model (3) can be modified to include the scintillation distortion as $y_k = \alpha_k e^{j\theta_k} + w_k \in \mathbb{C}$ (or its in-phase/quadrature equivalent) such that now the amplitude $\alpha_k = A_k \rho_{s,k}$ and phase $\theta_k = \theta_{d,k} + \theta_{s,k}$ incorporate the ionospheric disturbance (7). That is, *i*) the amplitude can be affected due to fades caused by the ionospheric propagation; and *ii*) the phase of the received signal contains the desired phase contribution due to receiver's dynamics, but also a phase noise due to the ionospheric scintillation event. When a standard carrier-phase tracking loop aims at tracking $\theta_{d,k}$ but instead tracks the combined $\theta_k = \theta_{d,k} + \theta_{s,k}$ phase, the degradation can be very large even causing loss-of-lock (Myer, Morton, & Schipper, 2017).

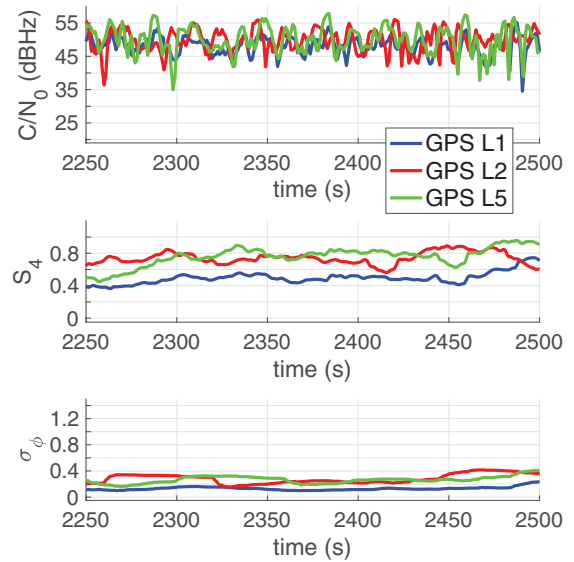


FIGURE 1 Moderate to strong (frequency dependent) equatorial amplitude ionospheric scintillation, with moderate phase scintillation. Event recorded over Hanoi, Vietnam, Spring 2015 [Color figure can be viewed in the online issue, which is available at wileyonlinelibrary.com and www.ion.org]

Notice that the S_4 and σ_ϕ indices offer no insight into the time correlatedness of the instantaneous phase and amplitude of scintillation observed on multiple frequencies. Recent studies have provided empirical evidence that the phase scintillation exhibits a high degree of correlation between different GNSS frequency bands (Carrano, Groves, Mcneil, & Doherty, 2012; Jiao, Xu, Morton, & Rino, 2016; Sokolova, Morrison, & Curran, 2015). For instance, there are articles showing that ionospheric scintillation effects are correlated among the L1, L2, and L5 frequency bands for the GPS system (Curran, Bavaro, Morrison, & Fortuny, 2015b). Interestingly, while phase distortions appear to be correlated, deep amplitude fades occur at different times on different frequencies, which stimulated research on multi-frequency receivers for ionospheric mitigation (Jiao et al. 2018; Vilà-Valls, Closas, & Curran, 2017a).

Figure 1 shows a strong to moderate amplitude-scintillation event, with moderate phase scintillation, at an equatorial region (Hanoi, Vietnam) recorded during spring 2015. The three GPS frequency bands are shown, showing that the effect on L1 frequency is smaller than on the L2 and L5 bands. That difference at different frequency bands is generally agreed based on experimental data (Jiao & Morton, 2015). At the same location, Figure 2 shows a severe scintillation event on both amplitude and phase, where we can observe deeper signal fades as reported by the CN_0 and σ_ϕ estimates.

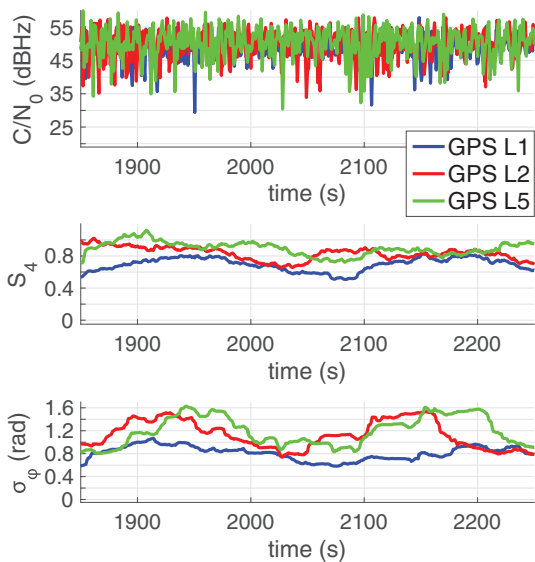


FIGURE 2 Severe equatorial amplitude and phase ionospheric scintillation. Event recorded over Hanoi, Vietnam, Spring 2015 [Color figure can be viewed in the online issue, which is available at wileyonlinelibrary.com and www.ion.org]

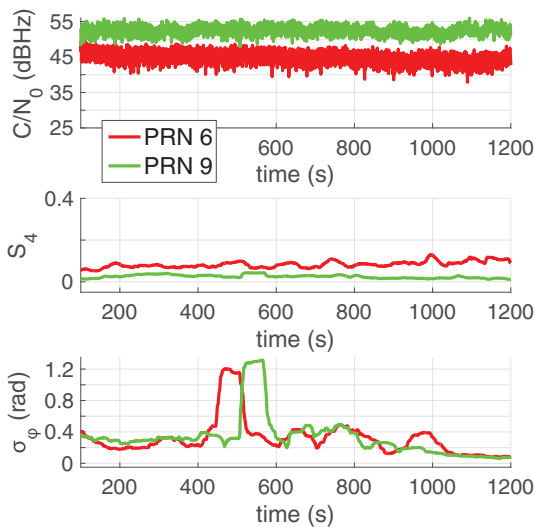


FIGURE 3 Single-frequency high-latitude ionospheric scintillation event recorded over Svalbard Islands, Norway, September 2017 [Color figure can be viewed in the online issue, which is available at wileyonlinelibrary.com and www.ion.org]

For the sake of completeness, Figure 3 shows a scintillation event at a high-latitude location (Svalbard Islands, Norway) recorded during September 2017. The recording involves single-frequency measurements, and the figure shows the indicators for two different satellites. Clearly, there is phase distortion appreciated around 400 – 600 seconds in the recording, as reported by the σ_ϕ estimate. Notice that in contrast with equatorial scintillation where both severe amplitude and phase variations may appear

(i.e., high S_4 and σ_ϕ), high-latitude scintillation typically only affects phase variations, that is, there are no deep amplitude fades (i.e., low S_4).

3 | SCINTILLATION DETECTION

The main purpose of scintillation detection is to warn users and systems about the presence of potentially harmful effects. Detection is indeed a key and preparatory step for both monitoring and mitigation, enabling them respectively: the observation of the phenomenon, being a precious source of information for understanding and modeling the upper layers of the atmosphere, and the application of countermeasures to reduce its impact on GNSS receivers performance. On top of this, accurate and timely detection is important to avoid recording potentially long sequences of GNSS data. Precious storage and network resources can be saved by properly identifying relevant scintillation events, especially for automatic and remote monitoring stations and in the case raw IF samples are stored (Linty, Romero, Dovis, & Alfonsi, 2015; Vikram, Morton, & Pelgrum, 2011).

For these reasons, accurate and early detection and classification of scintillation events is a very important feature for a number of applications, including space weather, atmospheric remote sensing, applications requiring high-precision GNSS, critical infrastructures relying on GNSS, and data collection systems. An overview and comparison of the detection techniques are provided hereafter. Table 1 summarizes pros and cons of each family of techniques.

It is interesting to notice that historically scintillation detection has been limited to stationary installations. pISMR providing scintillation indices are designed for static usage and perform properly in good sky visibility conditions and in low-multipath environments. The interest in scintillation detection on mobile receivers arises when detection is considered a preliminary step to mitigation. However, detection in dynamic conditions can be a challenge, especially considering the fragility of the indices estimation algorithms and of the definition of the detrending procedures. In principle, all the technique presented hereafter can be extended to the case of nonstationary users, as long as that the GNSS receiver in use supports dynamic conditions, has a good clock stability, and is able to provide the observables required with good quality. There is a trend in studying ionospheric monitoring via raw measurements from smartphones, as for example in Fortunato, Ravanelli, and Mazzoni (2019) where such measurements are processed to detect traveling ionospheric disturbances (TIDs); however, only a preliminary analysis has been carried out, and it showed limitations due to the poor quality of the measurements.

TABLE 1 Summary on the pros and cons of the different ionospheric scintillation detection strategies

	Pros	Cons	Real time
Manual visual inspection			
Inspection of scintillation indices and other observables (Jiao, Hall, & Morton, 2017a; Linty, Farasin, Favenza, & Dovis, 2019; Xu, Morton, Akos & Walter, 2015a).	Gives the ultimate accuracy and reliability and perfectly targets the scope of the analysis; allows an easy cross analysis of historical data and of any external aiding.	Performance depends on skills and experience of the operator; subject to human errors; requires costly and time consuming human effort; not automatic.	✗
Threshold based			
Scintillation indices threshold trigger (Dubey, Wahi, & Gwal, 2006; Linty, Dovis, & Alfonsi 2018; Linty et al. 2019; Taylor, Morton, Jiao, Triplett, & Pelgrum, 2012).	Very simple implementation; low computational burden.	Low detection accuracy; vulnerable to false alarms due to multipath; requires ISMR or detrending and filtering algorithms.	✓
Addition of elevation mask (Abadi, Saito, & Srigutomo, 2014; Favenza, Farasin, Linty, & Dovis, 2017) and C/N_0 (Curran, Bavaro, Morrison, & Fortuny, 2015b).	Simple; capable of reducing the false alarms due to multipath.	Significant risk of discarding important measurements and to miss the detection of events.	✓
Linear combination of scintillation indices and signal observables (Pelgrum et al., 2011; Vikram et al., 2011).	Simple; able to eliminate multipath.	Non-trivial tuning of parameters; limited scalability; non-negligible missed detection rate.	✓
Elevation-azimuth masks (Atilaw, Cilliers, & Martinez, 2017; Spogli et al., 2014).	Very good multipath rejection capabilities.	Long and complex preparation phase; low scalability, tuning bounded to the specific location.	✓
Non-indices based techniques			
Wavelet decomposition and transform based techniques (Fu, Han, Rizos, Knight, & Finn, 1999; Mushini, Jayachandran, Langley, MacDougall, & Pokhotelov, 2012; Ouassou, Kristiansen, Gjevestad, Jacobsen, & Andalsvik, 2016).	Overcome the problem of detrending using Butterworth filters; enhanced performance especially for phase scintillation; alternative scintillation indices are derived.	Computationally expensive; complex implementation; require phase measurements.	✗
Open-loop receivers (Romero et al., 2016).	Overcome the problem of detrending; does not require the tracking loops to be in lock condition.	Requires specific receiver implementation.	✗
Machine learning based			
SVM, Fourier Transform of signal time series (Jiao, Hall, & Morton, 2017b; Jiao, Hall, & Morton, 2017c).	High accuracy; resembles manual annotation by design; fully automatic; relies on common GNSS observables.	Requires large set of labeled data for the training phase; requires predetermined elevation mask.	✓
Decision Tree and correlator outputs (Linty et al., 2019).	Very high accuracy; resembles manual annotation by design; fully automatic; early detection of events; high-rate results.	Requires large set of labeled data for the training phase; vulnerable to the problem of over-fitting if the features are not properly chosen; requires access to correlator outputs.	✓

When evaluating the performance of scintillation detection, the major complication is given by false alarms induced by signal nuisances other than scintillation itself. Errors in the S_4 and σ_ϕ estimation can indeed affect the

scintillation detection process. Among the different error sources, multipath has a harmful impact on the quality of the amplitude-scintillation measurements, being that S_4 is a measure of the variability of the signal intensity

along time (De Oliveira Nascimento Brassarote, Souza, & Monico, 2018). The pattern induced by multipath reflected rays on the amplitude-scintillation index highly resembles the scintillation signature, in terms of periodicity and duration. This makes it very hard to distinguish them, especially when the characteristics of the environment surrounding the monitoring station are unknown. Such effects are particularly frequent for low-elevation satellites, where the number of multipath reflected rays increases, and at the same time, the CN0 is lower. It has also been proven that RFI causes unpredictable fluctuations of the value of the indices, further complicating the detection process (Qin & Dovis, 2018; Romero & Dovis, 2014). The most common strategy to reduce multipath-induced false alarms is indeed to filter all data from signals below a certain elevation mask, typically in the range $15 - 30^\circ$, as low-elevation satellites are naturally more prone to reflections (Spogli et al., 2014). However, applying a fixed-elevation cutoff angle leads to the potential loss of valuable data: relevant scintillation events might be completely missed out, significantly reducing the capability to depict the behavior of the ionosphere. At the same time, from the positioning perspective, a worse satellite's geometry is experienced, resulting in larger values of DOP.

3.1 | Visual inspection

Most of the approaches in the literature, especially in the works where scintillation indices are used as input to advanced studies, are based on manual visual inspection of S_4 and σ_ϕ , as provided by professional commercial ISMR. Time series of scintillation indices spanning intervals of several hours and typically including all satellites in view from all constellations and frequencies available are observed, and the presence of scintillations is empirically evaluated. To help the classification, users often rely also on assistance from other measurements and instruments, such as CN0, TEC, ROT, satellites azimuth and elevation, Solar flare detectors, or magnetometers. Also, the comparison with historical data can help in some situations, due to the unique regularity pattern of scintillations. As an example, fluctuations of S_4 due to multipath can be easily recognized on GPS signals by examining the same time series at regular intervals of one sidereal day (Axelrad, Larson, & Jones, 2005). The rate of the observation is typically one minute, and the detection resolution is of the order of tens of minutes. Even though lacking of scientific rigor, this approach assures the best detection performance. The main drawbacks are that it is time consuming, not automatic and subject to errors dependent on knowledge and experience of the person performing the task.

3.2 | Thresholding

More advanced and semi-automatized approaches are based on automatic event triggers, relying on the comparison of the value of the same scintillation indices with predefined thresholds. This approach is referred to as *threshold trigger* in Taylor et al. (2012) and as *Hard detection rule* in Linty et al. (2019), as it is a fully-automatized objective decision. Different thresholds can be defined for amplitude and phase scintillation, respectively, \mathcal{T}_{S_4} and $\mathcal{T}_{\sigma_\phi}$. A scintillation event is declared by the system when the indicator surpasses the threshold. When both S_4 and σ_ϕ are considered, then scintillation is declared present, at epoch n , if and only if:

$$S_4[n] > \mathcal{T}_{S_4} \quad \text{or} \quad \sigma_\phi[n] > \mathcal{T}_{\sigma_\phi}. \quad (10)$$

The performance clearly depends on the choice of the threshold, which in turn depends on different and complex factors including location, time, environmental conditions, and quality of hardware and of oscillator. Overly conservative thresholds result in large missed detections rates, whereas overly aggressive thresholds lead to large false alarm rates. Concerning amplitude scintillation, $\mathcal{T}_{S_4} = 0.4$ is chosen by many authors (Adewale et al., 2012; Aon, Othman, Ho, & Shaddad, 2015; Dubei, Wahi, Mingkhwan, & Gwal, 2005; Middlestead, 2017; Romero Gaviria, 2015); other works consider scintillation moderate in the range between 0.2 and 0.5 and strong above 0.5 (Jiao, Morton, Taylor, & Pelgrum, 2013a). Concerning phase scintillation, a common value is $\mathcal{T}_{\sigma_\phi} = 0.25$ rad (Dubey et al., 2006; Linty, Minetto, Dovis, & Spogli, 2018). Sometimes, the same authors consider different thresholds depending on the type of study being carried out: 0.15 and 0.26 rad for amplitude and phase scintillation, respectively, to detect events potentially causing a considerable impact on GNSS measurement accuracy and reliability (Jiao, Morton, Taylor, & Pelgrum, 2013b), while 0.12 and 0.1 rad, for studies on the ionosphere irregularity (Jiao, Morton, Taylor, & Pelgrum, 2013a).

Both the rate of the observation and the detection resolution are equivalent to a one-minute observation interval. The advantages are the simplicity, the low computational burden, and the low tuning requirements. However, it is prone to undesired and non-negligible false alarms, due to ambiguity between real scintillations and other kinds of nuisances, especially in the case of amplitude scintillation.

In order to reduce false alarms and missed detections due to multipath and other propagation errors, and to better characterize the scintillation phenomenon, more sophisticated techniques have been proposed. For instance, when measurements other than σ_ϕ and S_4 are available, additional masks can be applied to the signal.

It is quite common to apply an *elevation mask*; the majority of multipath-induced false alarms can be successfully removed by discarding signals below a certain elevation angle, at the expenses of the potential loss of relevant and useful information. A more advanced thresholding detection rule can be defined as follows: amplitude scintillation is present at epoch n if and only if:

$$S_4[n] > \mathcal{T}_{S_4} \quad \text{and} \quad \theta_{\text{el}}[n] > \mathcal{T}_{\theta_{\text{el}}}, \quad (11)$$

where the value of the elevation threshold $\mathcal{T}_{\theta_{\text{el}}}$ can be chosen depending on a *a priori* evaluation of the surrounding area. A typical value is 30° (Abadi et al., 2014; Jiao, Morton, Taylor, & Pelgrum, 2013a).

Similarly, further conditions can be defined on the CNO, so as to exclude measurements which are too noisy; or on the satellites azimuth, to counteract specific environmental signals obstructions. However, the definition of the corresponding \mathcal{T}_{C/N_0} is deemed more complex, as the CNO strictly depends on the receiver implementation. The value 37 dB-Hz has been proposed as threshold in some studies (Linty, Dovic, & Alfonsi, 2018; Linty, Farasin, Favenza, & Dovic, 2019), while other authors propose to use 40 dB-Hz (Curran, Bavaro, Morrison, & Fortuny, 2015a), or even 30 dB-Hz, corresponding to the tracking-loop sensitivity (Van Dierendonck, 2009). Pelgrum et al. (2011) proposed an event trigger based on a joint S_4 and CNO threshold, in the form:

$$S_4 > 1.075 - C/N_0 \cdot 0.01875, \quad (12)$$

where CNO is in dB-Hz and 0.01875 is in units of $(\text{dB-Hz})^{-1}$. According to Vikram et al. (2011), no false alarms were detected using this technique over a six-day data collection, at the expenses of a high missed detection rate (4 events detected out of 25), especially in the presence of phase scintillation.

An extension of this, taking into account also the σ_ϕ and satellites elevation was proposed in Vikram et al. (2011). To reduce the multipath effects, all entries below 30° were *a priori* eliminated. Scintillation is then declared present if one of the two conditions holds:

$$S_4 > -9.09 \cdot 10^{-4} \theta_{\text{el}} + 0.1373 \quad (13)$$

$$\sigma_\phi > -6.36 \cdot 10^{-4} \theta_{\text{el}} + 0.1091 \quad (14)$$

with θ_{el} expressed in degrees. This technique was further refined by adding a third condition on the satellites azimuth, based on empirical considerations on a set of data, and selecting the thresholds according to a user-specified false alarm rate and on a manual visual-based

scintillation detection. A disadvantage of such an approach is that it relies on a minimization process on a certain distribution of data and does not scale well for different spatial and temporal observations. Furthermore, the same study of the authors reveals high false alarm rates. In general, despite a difference in the detection results that has been observed between summer and winter, this is negligible and a separate threshold setting for winter and summer is not necessary (Taylor et al., 2012).

In order to better filter data affected by multipath, more advanced masks can be defined. As multipath effects are location dependent, the environment surrounding the receiver can be characterized, to avoid losing valuable data by setting predetermined filtering masks. A location-specific azimuth-dependent elevation mask has been developed in Atilaw et al. (2017).

Another possible way to distinguish scintillation events from multipath is to rely on historical data and on the repeatability of GNSS satellites visibility. For instance, in the case of the GPS constellation, it is generally assumed that the GPS orbits repetition equals the sidereal day (23 hours, 56 minutes, and 4 seconds), although the precise amount of time shift may vary somewhat depending on the true satellite orbit (Axelrad et al., 2005). Therefore, also, multipath effects follow the same repeatability. The pattern induced by multipath on the S_4 can be considered deterministic and is observed with regularity, contrary to true scintillation events, which are inherently random. Spogli et al. (2014) proposed a method to filter out spurious data, including multipath affected signals, based on an “outliers analysis.” Such an approach can reduce the data loss from 35 – 45% to 10 – 20%.

3.3 | Non-scintillation indices-based techniques

Approaches based on the sole analysis of the scintillation indices share a common drawback. S_4 and σ_ϕ , despite being widely recognized, overlook higher moment characteristics of the signals (Jiao, Hall, & Morton, 2017a). Their computation requires averaging and detrending operations and, in general, algorithms with complex tuning, which are time consuming, computationally expensive, and potentially introduce heavy artifacts, thus altering the scintillation detection process (Mushini et al., 2012). In particular, although detrending the phase by means of a Butterworth filter is the *de facto* standard (Van Dierendonck, Klobuchar, & Hua, 1993), many authors have shown limitations when dealing with polar scintillations, related to the choice of the filter cutoff frequency, which should be related to the local features of the ionosphere (Forte, 2005; Mushini et al., 2012; Ouassou et al., 2016).

A wrong and non-adaptive cutoff frequency ultimately alters the value of the traditional indices up to the point in which the scintillation detection is completely mistaken. Furthermore, detection based on fixed thresholds can be misleading: a hard classification based on the definition of thresholds (no scintillation, moderate scintillation, strong scintillation) determines abrupt and sudden classification, often irrespective of the true physical process determining the event. Furthermore, transient phases of the events can be lost, causing a delay in the detection alert (Linty et al., 2019), while weak events with high variance can be missed. A fuzzy indication system giving a more reasonable expression of the scintillation depth has been proposed, to overcome the ambiguity existing in the numerical and linguistic definitions of scintillation intensity (Fu et al., 1999).

Alternatives to detection rules based on scintillation indices and thresholds usually exploit dedicated receiver architectures and possibly complex and computationally expensive operations. For these reasons real-time detection is usually not possible. One of the first techniques based on alternative analysis was proposed in Fu et al. (1999) and is based on wavelet decomposition. According to the authors, scintillation-related signal features can be effectively detected or extracted by transforming the time domain scintillation signals by means of orthonormal and compactly supported wavelet bases. Wavelet-based detrending has also been proposed in Mushini et al. (2012). Alternative scintillation indices, based on non-parametric local regression with bias Corrected Akaike Information Criteria (AICC) have been proposed by Ouasson *et al.*, reducing the computational load of wavelet analysis and superior handling of discontinuities (Ouassou et al., 2016). Recently, the Adaptive Local Iterative Filtering (ALIF) method has been proposed to analyse phase time series, improving scale resolution with respect to wavelet transform (Piersanti et al., 2018).

When dealing with amplitude scintillation only, the analysis of CN0 allows detection of anomalous variations in the signal amplitude. In this case, it is even harder to distinguish between real scintillation and other impairments. However, the CN0 is a measure largely available in any GNSS receiver, including mass-market and non-professional devices, making CN0-based techniques cheap, accessible, and applicable also to historical data. In Miriyala, Koppireddi, and Chanamallu (2015), CN0 time series of GNSS data are decomposed exploiting adaptive time-frequency methods. In particular, the technique denoted complementary ensemble empirical mode decomposition showed good detection results.

More recently, and thanks to the widespread availability of raw IF samples of GNSS signals for scintillation monitoring (Cristodaro, Dovic, Linty, & Romero, 2018; Lachapelle & Broumandan, 2016), other approaches have been pro-

posed, directly looking at lower processing stages of the receiver. The received signal samples contain information about scintillation, although buried in the noise floor. After removing the deterministic components of the signal (carrier frequency, modulating codes, and navigation message), and by filtering out noise exploiting averaging techniques, the contribution of scintillation can be isolated. An open-loop approach was proposed in Romero et al. (2016) and Linty and Dovic (2019); a metric alternative to the S_4 was suggested to detect amplitude scintillation, based on the evaluation of the statistical properties of the histogram of the received samples. Different techniques were evaluated, such as skewness and goodness of fit, obtaining high detection, low false alarm, and low missed detection rates when compared to the S_4 -based thresholding. Despite requiring a dedicated receiver architecture, this approach is insensitive to the degradation of the results due to strong scintillations, which might impact on the receiver tracking loops and thus falsify the traditional detection.

3.4 | Machine learning

Recent studies have proposed machine learning techniques for automatically detecting scintillation events. A machine learning process refers to the ability of solving a task by processing right features describing the domain of interest, according to a model built upon training on a set of historical data, which in the case of supervised learning are pre-labelled by manual annotation. More details about machine learning can be found in general purpose books, such as Flach (2012).

The selection of the set of features to be used in the training and in the classification tasks is the key aspect of machine learning algorithms. A clear strategy envisages the use of high-level observables, including the amplitude- and phase-scintillation indices, the signal CN0, and the satellites' elevation and azimuth. This was first done exploiting SVM for the detection of amplitude scintillation in Jiao, Hall, and Morton (2016) and Jiao, Hall, and Morton (2017a). The algorithm was trained using a large amount of real scintillation data, manually labelled, and showed detection accuracy in the range 91-96%, outperforming other triggering systems analyzed. Some benefits were observed by including a further feature, corresponding to the Fourier Transform of the S_4 time series along an observation period of three minutes. A similar approach, targeting phase scintillation, was presented in Jiao, Hall, and Morton (2017b) and Jiao, Hall, and Morton (2017c), leading to detection accuracy around 92%.

Other works propose to use decision tree algorithms and low-level signal observables, such as the in-phase and quadrature correlation outputs of the receiver tracking

loop (Favenza et al., 2017; Linty et al., 2019). The authors proved that the amplitude-scintillation detection accuracy is as good as 96.7% when S_4 , CN0, and satellite elevation are used as features, but increases to 98.0% when using only correlator outputs and their combinations. Results further improve (99.7%) when using random forest algorithms at the expense of large computational loads. The authors also show how this approach is able to reduce the rate of false alarms due to the ambiguity between scintillation and multipath typical of the approaches based on the analysis of the S_4 . Decision tree algorithms are also able to detect the transient time before and after the strongest phase of an event, thus providing an early run-time alert. Another advantage is that by exploiting the high-rate correlator outputs, a finer time resolution in detection is obtained. Furthermore, avoiding the use of the scintillation indices prevents any issue with the detrending and filtering processes. It is also important to mention that while the training phase to build the model can be computationally demanding, the decision phase is typically simple enough to be done in real time and with no impact on performance.

More recently, semi-supervised scintillation detection based on DeepInfomax technique has been proposed (Franzese, Linty, & Dovis, 2020). The method shows a classification accuracy in line with Linty et al. (2019), while reducing the amount of time required to manually label the training dataset, thus overcoming the drawbacks of supervised algorithms and advancing towards realistic deployment of machine learning-based scintillation detection. More generally, in Rezende et al. (2010), the authors propose a survey of data mining techniques for the prediction of ionospheric scintillations, relying on the observation and integration of GNSS receivers, other sensors, and online forecast services. This approach relies on external data sources and instruments.

4 | SCINTILLATION MONITORING

Ionospheric scintillation monitoring is crucial when it comes to understanding the physics behind the process. Among the various options to accomplish such monitoring, the use of GNSS signals is widely considered because of their global coverage and the availability of multiple frequencies (Beach & Kintner, 2001; Humphreys et al., 2009). At a glance, a GNSS-based ionospheric monitoring station tracks code and carrier phase from the in-view satellites (either one-by-one or collectively) and isolates the ionospheric effects with perfect knowledge of the receiver's location, orbital parameters, and related quantities (Lee, Morton, Lee, Moon, & Seo, 2017). Therefore, monitoring receivers have, in general, demanding specifications in

their hardware and processing components. Particularly, estimates of ionospheric phase and amplitude traces are typically obtained from the receiver's carrier phase (after correcting for the receiver's location-related terms) and prompt correlator outputs, respectively. Arguably, these observations are limited by the ability of the monitoring receiver to track the GNSS signals, particularly in a scintillation event (Banville & Langley, 2013; Ghafoori, 2012). As a consequence, one of the main challenges in monitoring scintillation is to distinguish among ionospheric anomalies, receiver, and environmental artifacts. For instance, multipath fading might be regarded as amplitude scintillation and carrier-phase cycle slips could be confused with quick-phase fluctuations. Therefore, it is paramount to have highly reliable GNSS receivers for monitoring. Such resilience comes from exploiting accurate knowledge of the receiver's location, GNSS time, and ephemerides.

There are several deployed networks of monitoring GNSS receivers, typically in scintillation-active regions such as equatorial or high-latitude locations. ISMR architectures and solutions vary depending on the team designing and deploying the receivers, for which several possible architectures for implementing ionospheric monitoring networks exist in the literature. Stations that were - or currently are - deployed include the architecture in Beach and Kintner (2001), the works in Curran, Bavaro, and Fortuny-Guasch (2014) and Curran, Bavaro, Fortuny-Guasch, and Morrison (2014); Curran, Bavaro, Morrison, and Fortuny-Guasch (2014) report an open-loop vector-receiver scheme for monitoring scintillation events using a multitude of constellations and frequencies; in parallel, multi-frequency monitoring stations are as well reported in Yin, Morton, and Carroll (2014), Xu, Morton, Akos, and Walter (2015b), and Xu and Morton (2015, 2018), where semi-open-loop schemes are explored; in contrast, a closed-loop receiver architecture for monitoring was proposed in Vilà-Valls, Fernández-Prades, Curran, and Closas (2017). ISM stations are relevant in many applications involving critical infrastructures (Jakowski et al., 2012). Notably, its relevance in aircraft landing systems through GBAS is crucial for enabling differential GNSS techniques. In this context, networks of ISM stations are deployed in order to provide reliable ionospheric corrections (Fujiwara & Tsujii, 2016; Pullen, Park, & Enge, 2009; Yoon, Kim, Pullen, & Lee, 2019).

Noticeably, those ISM deployment efforts have led to the development of scintillation models, such as those mentioned in Section 2.2, that are currently used in the development of detection and mitigation algorithms for GNSS receivers, as well as to better understand the physics behind the ionospheric scintillation process.

5 | SCINTILLATION MITIGATION

Ranging from classic delay/phase-locked loop (DLL/PLL) tracking architectures and heuristic decision rules to advanced signal-processing techniques, several different strategies exist for scintillation mitigation at the receiver level. In this section, we provide a comprehensive review of the state of the art, with emphasis on the signal-processing aspects of the different alternatives.

Among the different ionospheric scintillation propagation conditions, obviously, the strong scintillation case is the one really compromising receiver operation. One of the major challenges of severe scintillation is the so-called canonical fades, which results in a combination of strong fading and rapid phase changes in a simultaneous and random manner (Humphreys et al., 2009; Kintner et al., 2009). From a synchronization standpoint, counteracting such an effect is very challenging, because the receiver has to track the faster phase changes using the worst signal level (Humphreys, Psiaki, & Kintner, 2005). This may lead the receiver to momentarily lose carrier synchronization, resulting in either cycle-slips or loss of lock. In the event of multiple cycle slips the quality of carrier-phase positioning can be significantly degraded to the point where it might not be available. For high-precision receivers, a key point is to mitigate the scintillation effects in order to have accurate carrier-phase observables. If several satellites are simultaneously affected by strong scintillation, positioning may be no longer continuously available, being a hazardous situation in safety critical and high-integrity applications. Taking into account the importance of having reliable carrier-phase measurements in advanced receivers and precise positioning applications, the main goal to counteract ionospheric scintillation disturbances is to mitigate its impact on the signal carrier phase. It is worth saying that even if moderate scintillation may not cause loss-of-lock in standard receivers, it may lead to useless phase observables in high-precision receivers.

An overview and comparison of the mitigation techniques are provided hereafter. Table 2 summarizes pros and cons of each family of techniques.

5.1 | Single-frequency synchronization

Traditional single-frequency synchronization (i.e., considering each satellite to receiver link independently) relies on well-known closed-loop DLL/PLL architectures (Kaplan, 2006) (see Section 2). When dealing with scintillation mitigation, state-of-the-art solutions attempt to render these classical approaches more robust, typically using heuristic adjustments (López-Salcedo, Peral-Rosado, & Seco-Granados, 2014; Yu et al., 2006). For instance, Skone

et al. (2005) proposed an adaptive bandwidth PLL, which was coupled to a prediction model in Tiwari, Skone, Tiwari and Strangeways (2011). Other approaches rely on the combination of FLLs with PLLs (Fantinato, Rovelli, & Crosta, 2012; Mao, Morton, Zhang, & Kou, 2010; Zhang & Morton, 2009), extending the coherent integration time (Kassabian & Morton, 2014) and coupling with inertial sensors or Doppler-aided solutions (Chiou, 2010; Chiou, Gebre-Egziaber, Walter, & Enge, 2007; Chiou, Seo, Walter, & Enge, 2008). These techniques are somehow designed to avoid the loss-of-lock, with the main goal being to maintain a correct DLL tracking under scintillation conditions, which is only useful in standard code-based receivers. But, the limitations of standard locked-loop architectures are inherited by all these methods (Vilà-Valls, Closas, Navarro, & Fernández-Prades, 2017).

Some contributions have recently shown that an optimal filtering approach based on Kalman filtering (KF) (Anderson & Moore, 1979) provides better performance and robustness to scintillation (Barreau, Vigneau, Macabiau, & Deambrogio 2012; Humphreys, Psiaki, & Kintner, 2005; Macabiau et al., 2012; Zhang, Morton, Van Graas, & Beach, 2010), being nowadays the performance benchmark for the development of new methodologies. To avoid the complexity of the optimal Kalman gain computation (which is obtained from the prediction and estimation noise covariances, together with the system noise covariance matrices), these typically consider a constant gain KF implementation and then lose the optimality of the filter. Because the actual receiver working conditions are unknown to some extent, solutions based on adaptive KF (AKFs) have been studied in Zhang, Morton, and Miller (2010); Won, Eissfeller, Pany, and Winkel (2012); Won (2014); Susi, Aquino, Romero, Dovis, and Andreotti (2014); Susi, Andreotti, and Aquino (2014); and Xu, Morton, Jiao, and Rino (2017), which aim at sequentially adapting the filter parameters. Notice that the correct estimation of both noise covariance matrices is not possible due to identifiability issues (Vilà-Valls, Closas, & Fernández-Prades, 2015a), then typically only the measurement noise is adjusted. Some of the standard noise estimation techniques based on covariance matching and the autocorrelation of the innovation function (Duník, Straka, Kost, & Havlík, 2017) were evaluated in Vilà-Valls, Fernández-Prades, Closas, and Arribas (2017) and a new approach based on Bayesian covariance estimation in LaMountain, Vilà-Valls, and Closas (2018); the latter being a very promising approach.

From a signal-processing perspective, all the PLL/KF-based solutions above claim robustness against ionospheric scintillation, but this is done only by ensuring a certain robustness against cycle slips and loss-of-lock (i.e., increasing the noise uncertainty under scintillation

TABLE 2 Summary on the pros and cons of the different ionospheric scintillation mitigation strategies

Single-frequency	Pros	Cons
Std PLL-based solutions (Kassabian & Morton, 2014; Skone et al., 2005; Yu et al., 2006).	Modification of standard PLL architectures, then easy to implement, tune and use. These techniques can be used for a mild receiver scintillation protection.	Not reliable for moderate/severe scintillation conditions. These techniques inherit the std PLL limitations and do not solve the mitigation problem.
Combined/Aided Loops (Chiou, 2010; Fantinato et al., 2012; Mao et al., 2010; Zhang & Morton, 2009).	Using well-known architectures, this approach improves the robustness w.r.t. standalone PLL-based solutions and is easy to implement in standard receivers.	These solutions still remain suboptimal when compared to adaptive KF-based techniques. As in the previous case, tracking the complete phase, they do not solve the EvM.
Std KFs (Humphreys et al., 2005; Macabiau et al., 2012; Zhang et al., 2010).	Improved robustness to loss-of-lock and cycle slips w.r.t. std/combined locked loops. Can be combined with external aiding.	To be optimal they require a perfect knowledge of the system working conditions, and in general, do not solve the EvM issues.
Adaptive KFs (Susi, Andreotti, & Aquino, 2014; Xu et al., 2017; Zhang, Morton, & Miller, 2010).	Solve the limitations of std KFs and provide the best standard (not using scintillation models) single-frequency solution.	AKFs track the complete signal phase, then have the same fundamental problem than the previous 3 cases, not being able to decouple the scintillation phase contributions.
AR-based KFs (Vilà-Valls et al., 2018; Vilà-Valls, Fernández-Prades, & Curran, 2018).	Embedding the scintillation into the filter formulation solves the EvM problem, then being robust to severe conditions and reducing loss-of-lock and cycle slips.	Increased computational complexity, need for adaptive system and scintillation model parameters estimation, and still not tested in a complete receiver chain.
Multi-frequency (MF)	Pros	Cons
MF PLL/KF-based solutions (Carroll, Morton, & Vinande 2014; Najmafshar et al., 2013; Psiaki et al., 2007; Seo and Walter, 2014).	Increased robustness when compared to their single-frequency counterpart, and relatively easy to implement and use.	These techniques have the same fundamental problems than both single-frequency PLL and AKF approaches detailed above.
MF AR-based KFs (Vilà-Valls et al., 2017a).	This solution improves both the single-frequency AR-based approach and std MF architectures robustness, being a promising solution for high-precision receivers.	Higher computational complexity, require data wipe-off to avoid the discriminators, and must include adaptive system and scintillation parameter estimation techniques.
Multi-freq/multi-system	Pros	Cons
Position-level mitigation (Aquino et al., 2007; Myer et al., 2017; Strangeways and Tiwari, 2013; Warnant et al., 2009).	Easy to implement in mass-market receivers and providing good performance with high satellite visibility (open-sky conditions).	Not exploiting signal-processing techniques, and possibly providing a degraded system performance with low satellite visibility.
Vector-tracking methods (Marçal et al., 2017; Peng, 2012; Sousa and Nunes, 2014b).	Useful under mild scintillation conditions to robustify the PVT solution.	Under severe conditions VTLs do not solve the mitigation problem.

conditions, so that the KF relies more on the LOS phase prediction model than on the current observation). But such an approach does not provide an effective mitigation of the harsh propagation conditions of interest. The question is how to design a method which minimizes the LOS carrier-phase estimation error. This leads to the estimation versus mitigation (EvM) dichotomy (Vilà-Valls et al., 2015a), which implies that a filter tracking the complete signal phase is not able to decouple the phase contribution due to the receiver dynamics of interest from

the phase changes due to scintillation. A new approach to overcome these limitations was first proposed in Vilà-Valls et al. (2013) and later extended in Vilà-Valls, Closas, and Fernández-Prades (2015b) and Vilà-Valls et al. (2015a, 2018), where the scintillation physical phenomena is mathematically modeled as an autoregressive (AR) process, and embedded into the state-space formulation, which allows decoupling both phase contributions of interest. This method has been tested using both synthetic and real data, providing very promising performance results.

Recently, to increase robustness in time-varying scenarios, adaptive AR parameter estimation techniques have been considered in Vilà-Valls, Fernández-Prades, Closas, and Arribas (2017) and Fohlmeister et al. (2018), showing that the approach in Vilà-Valls, Closas, Fernández-Prades, and Curran (2018) is the latest trend on single-frequency scintillation mitigation, and must be seen as the performance benchmark for the derivation of new scintillation mitigation strategies.

5.2 | Multi-frequency synchronization

It is known that the ionospheric scintillation effects are frequency and latitude dependent (see Section 2). For instance, while in equatorial regions, a receiver experiences severe amplitude scintillation, and in high latitudes, the phase scintillation is the dominant part. Multi-frequency receivers (i.e., using GPS L1 C/A, L2 and L5) try to exploit the different scintillation characteristics at different frequency bands, with the aim to exploit the fact that not all the frequencies are equally degraded at the same time. As an example, deep amplitude fades in equatorial scintillation have low correlation (Seo, 2010), the reason why multi-frequency processing increases the robustness to scintillation (Carroll et al. 2014; Najmafshar, Ghafoori, & Skone, 2013; Psiaki, Humphreys, Cerruti, Powell, & Kintner, 2007; Seo & Walter, 2014). As stated for the single-frequency case, relying on standard multi-frequency PLL/KF-based architectures is not a good approach from a signal-processing perspective, because the filters track the complete phase of the signals, losing the capacity to effectively isolate the LOS and scintillation phase contributions.

The AR-based scintillation modeling within a KF-like architecture in Vilà-Valls, Closas, Fernández-Prades, and Curran (2018) was extended to the multi-frequency case in Vilà-Valls, Closas, and Curran (2017) and Vilà-Valls, Closas, and Curran (2017a), using a multi-frequency state-space model formulation and a multivariate AR scintillation model. It was shown that exploiting both multi-frequency measurements and the scintillation approximation embedded into the filter improves the overall performance and robustness.

5.3 | Multi-frequency/Multi-satellite solutions

There has been substantial research on combined multi-frequency/multi-satellite receivers to counteract scintillation (Lin, Lachapelle, & Souto Fortes, 2014). The easiest

way to cope with such disturbance is to properly modify the navigation solution, typically weighting the pseudorange observables affected by scintillation (Aquino et al., 2007; Strangeways & Tiwari, 2013; Warnant et al., 2009), but from a signal-processing perspective, more sophisticated approaches can be considered. At the position level, another possible solution is to switch between phase and pseudorange observables when an event is detected (Myer et al., 2017).

In order to address some of the limitations of standard scalar synchronization techniques, mainly for weak signal environments and high-dynamics scenarios, several vector synchronization architectures (VTL) have been proposed in the last two decades (Giger, Henkel, & Günther 2009; Henkel, Giger, & Gunther, 2009; Lashley, Bevely, & Hung, 2009; Marçal & Nunes, 2016; Spilker, 1996). These solutions take advantage of the joint multi-channel (vector) processing, then making possible the meaningful exchange of information between channels. The goal is that channels under benign nominal conditions help the channels, which are corrupted by harsh propagation conditions, lowering the tracking threshold and thus increasing the satellite availability. These vector architectures have been shown to provide better position accuracy and increased robustness under non-nominal conditions w.r.t. standard scalar architectures. It is not the goal of this article to describe in detail the different vector-tracking architectures (i.e., vector DLL, vector DFLL, vector PLL, differential VPLL, partitioned vector tracking, etc.). Refer to the references provided and references therein for a deeper insight on pros and cons of the different approaches available in the literature.

These vector-tracking techniques have also been recently evaluated under ionospheric scintillation propagation conditions (Deambrogio & Macabiau, 2013; Marçal, Nunes, & Sousa, 2016, 2017; Peng, 2012; Sousa & Nunes, 2014a, 2014b; Xu, Jade Morton, Jiao, Rino, and Yang, 2018) in order to robustify the overall navigation solution. Even if the performance degradation of vector architectures under ionospheric scintillation is smaller when compared to standard (DLL/PLL) scalar-tracking techniques, including scintillation-affected satellites into the vector solution is not a good option. Using scintillation detection techniques to discard those satellites affected by scintillation from the navigation solution seems to be a better option, but this is not possible in situations with low satellite visibility. Then, from a signal-processing perspective, vector synchronization strategies may not be a good approach, at least in their current status. Notice that the advanced signal-processing techniques described in Sections 5.1 and 5.2 can also be used in multi-frequency/multi-satellite configurations to improve the overall system performance, taking the best of both worlds.

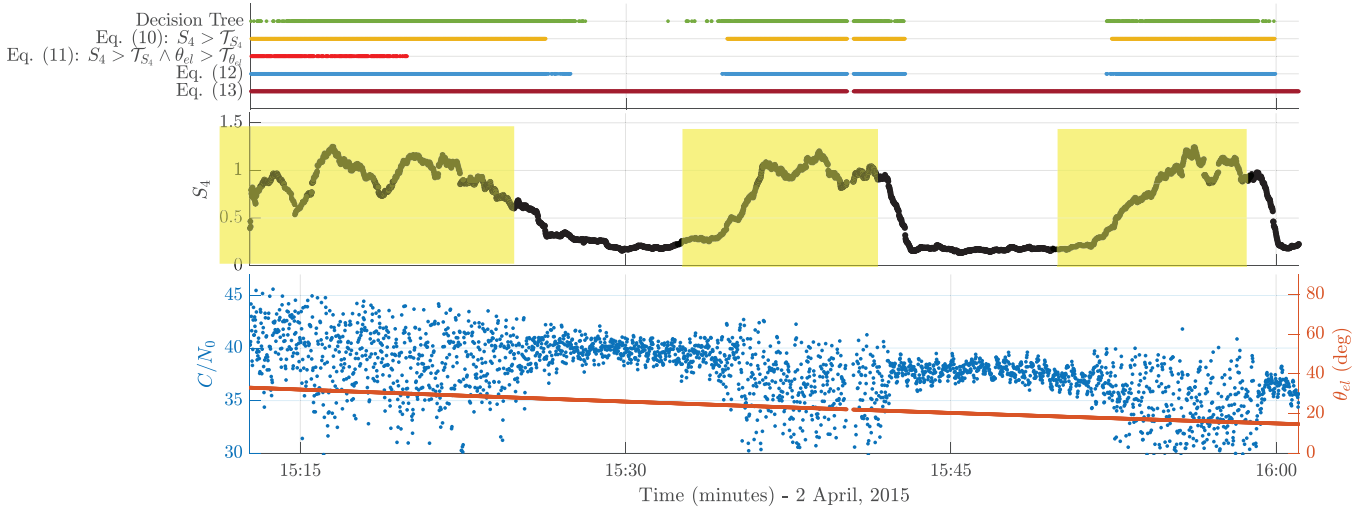


FIGURE 4 Example of amplitude detection results on data captured on April 30, 2015, GPS PRN 30, L1 C/A [Color figure can be viewed in the online issue, which is available at wileyonlinelibrary.com and www.ion.org]

6 | RESULTS ON GNSS IONOSPHERIC SCINTILLATION DETECTION, MONITORING, AND MITIGATION

To support the discussion on the different signal-processing methods described in previous sections, we show detection, monitoring, and mitigation results for some representative scenarios. The main goal is to provide further insights, but it is out of the scope to conduct an exhaustive analysis.

6.1 | Examples of scintillation detection

An overview of scintillation detection results is provided in this section. The techniques described in Section 3 are applied on the example datasets presented in Figures 2 and 3. Only qualitative results are shown, as a complete statistical analysis on detection techniques would require to consider a much larger input dataset, representative of any possible physical and environmental conditions. Moreover, each of the techniques presented targets a specific monitoring need, thus it is not possible to compare them in a unified way. For these reasons, the figures shall be considered illustrative and not conclusive; the readers interested can delve into the appropriate references provided.

Figure 4 reports a time series of S_4 , CN0 and elevation of GPS PRN 30 on April 2, 2015 at equatorial latitudes. The yellow boxes throughout the S_4 trace identify the portions of data affected by amplitude scintillation, according to a manual visual inspection of the dataset. Even though after minute 15:22 the elevation is lower than 30° , the analysis of historical data and of the station environment

assures that multipath cannot be held responsible for such an increase of the amplitude-scintillation index. The detection results are depicted in the top panel of the figure. The simple thresholding rule of Equation (10) marks as scintillation all the points for which S_4 is larger than $\mathcal{T}_{S_4} = 0.4$. Carefully analyzing, it appears that the rule fails in detecting the exact start and end of each event. When the mask on the elevation is also applied, as defined in Equation (11), all points after minute 15:22 are discarded, resulting in a large missed detection rate. The detection rule of Equation (12) shows very good results, well aligned with the event visual inspection. On the contrary, the results of Equation (13) mark as scintillation all the points of the time series. This is probably due to the high noise floor of the S_4 estimate, potentially due to the bad quality of hardware used for the data collection. A slight modification of the equation would be required, performing a calibration on data not affected by scintillation. The green line reports the detection results of a decision tree machine learning technique using as observables the correlator outputs, as proposed in Linty et al. (2019). The training phase was performed on other data captured at the same station during different events.

Similarly, qualitative results of the phase-scintillation detection methods are reported in Figure 5. σ_ϕ , CN0 and elevation time series of GPS PRN 6, on September 8, 2017, at high latitudes, are reported. As above, the yellow box marks the start and end of the phase-scintillation event, according to visual inspection. The hard rule of Equation (10) is reported for two different thresholds, $\mathcal{T}_{\sigma_\phi} = 0.25$ rad and $\mathcal{T}_{\sigma_\phi} = 0.4$ rad. In the first case, the detection result almost matches the performance of the manual inspection, but misses a few points, which despite showing a σ_ϕ lower than the threshold are clearly part of the same scintillation

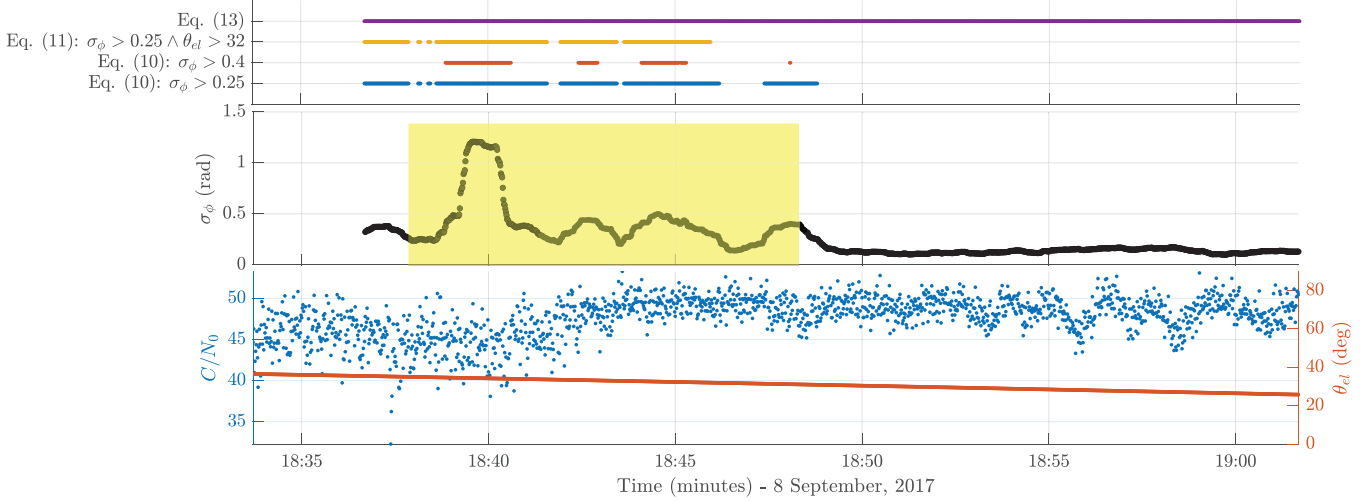


FIGURE 5 Example of phase detection results on data captured on September 8, 2017, GPS PRN 6, L1 C/A [Color figure can be viewed in the online issue, which is available at wileyonlinelibrary.com and www.ion.org]

event. Adding also the elevation mask, according to Equation (11), brings no benefits; however, this is due to the fact that no multipath is present in this specific data acquisition. The rule defined in Equation (13) is also reported, but as in the case of amplitude scintillation, it fails due to the high noise floor of the σ_ϕ estimation. Also, in this case, a calibration phase would be required.

It is clearly not possible to identify the optimum technique, according to detection results of a single event, and with no specification about the target application. High-end receivers have different requirements, in terms of scintillation detection, compared to mass-market receivers and to receivers for space weather monitoring. Similarly, certain applications require the detection of events which are harmful for the capability of the GNSS receiver to produce a correct position estimate; other applications require the detection of events significant under a physical point of view. In general, improved processing capabilities allow nowadays the design and implementation of very advanced detection schemes, reaching very high detection rates and low false alarms.

6.2 | Example of high-latitude scintillation monitoring

As already stated, ionospheric scintillation monitoring is of paramount importance for several scientific applications (Coster, Gaposchkin, & Thornton, 1992; Doherty, Coster, & Murtagh, 2004; Goncharenko, Chau, Liu, & Coster, 2010; Goncharenko, Coster, Chau, & Valladares, 2010). The main limiting factor for the use of low-cost mass-market GNSS receivers for this purpose (i.e., to avoid high-cost professional dedicated ISMR with very stable clocks and

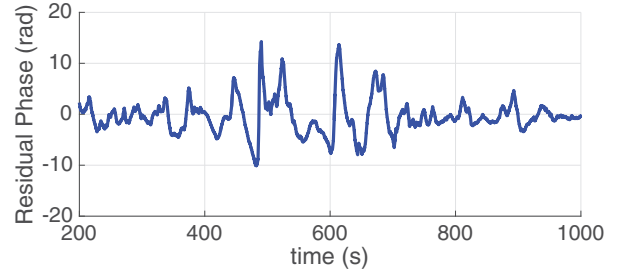


FIGURE 6 Real ionospheric scintillation event recorded over Svalbard Islands, Norway, September 2017. The scintillation-induced phase variations to be estimated are shown for $T_I = 10$ ms [Color figure can be viewed in the online issue, which is available at wileyonlinelibrary.com and www.ion.org]

perfectly known position) is the clock-induced phase errors. Considering the architecture proposed in Vilà-Valls, Closas, and Curran (2017a), we show new results for a high-latitude scintillation event, recorded in September 2017 over Longyearbyen, at the Svalbard Islands, Norway (Linty, Minetto, DAVIS, & Spogli, 2018), using a customized receiver developed by the NavSAS group of Politecnico di Torino (Cristodaro et al., 2018). As a low-cost receiver clock example, we consider a typical temperature-compensated crystal oscillator (TCXO), for which we measured the clock-phase-induced errors. The characterization of the scintillation event is shown in Figure 3 (PRN 9) where there is no amplitude scintillation but phase scintillation is clearly present, as expected for a high-latitude ionospheric scintillation event. In this exemplary case, the phase residual to be tracked is shown in Figure 6. Recall that this phase residual is the output of the DLL prompt correlator, then it depends on the integration time, i.e., $T_I = 10$ ms in this case. Notice that this integration time is purposely

TABLE 3 RMSE (rad) for the estimation of a high-latitude scintillation phase event, with and without clock-phase compensation

	Scint phase	Scint + Comp. Clock	Scint + Clock
RMSE	0.0664	0.0864	1.7257

chosen to show a challenging scenario, for instance compared to a $T_I = 1$ ms choice, which would induce slower phase variations and thus be easier to track at the receiver.

At the receiver, we consider a nominal $C/N_0 = 40$ dB-Hz and a coherent integration time of $T_I = 10$ ms. The root-mean-square error (RMSE) for the estimation of the TCXO clock-induced phase variations (i.e., computed from a scintillation-free satellite link) is 0.0574 radians. This estimated clock phase is used to compensate the clock error in the scintillation affected satellite link. In Table 3, we show the monitoring capabilities of the AR-based KF. The different values correspond, left to right, to the RMSE for the estimation of the scintillation phase variations without any clock-phase error, the RMSE for the estimation considering a compensated clock from the scintillation-free satellite link, and the RMSE for the estimation without compensating the clock-phase errors. It is clear that a bad quality clock has a huge impact on the receiver, not being able to correctly estimate the scintillation phase of interest because the filter tracks the complete phase (scint + clock). But correctly using a clock estimation procedure provides a good scintillation phase estimate, which opens the door for low-cost monitoring architectures, boosting new scientific applications.

6.3 | Example of adaptive multi-frequency severe equatorial scintillation mitigation

To close the loop and give a better insight on the synchronization performance, we show new results for a robust scintillation mitigation example. We assess the performance of different methods using real equatorial data recorded during high ionospheric activity. The real triple-frequency (L1, L2 and L5) amplitude- and phase-scintillation time series are obtained from the Joint Research Centre (JRC) Scintillation Repository, recorded over Hanoi in March and April 2015. To obtain the clean ionospheric scintillation time series, a multi-frequency open-loop software receiver was used for post-processing the original datasets (Curran, Bavaro, Morrison, & Fortuny, 2015a, Curran, Bavaro, Morrison, & Fortuny, 2015b). We propose a new adaptive multi-frequency architec-

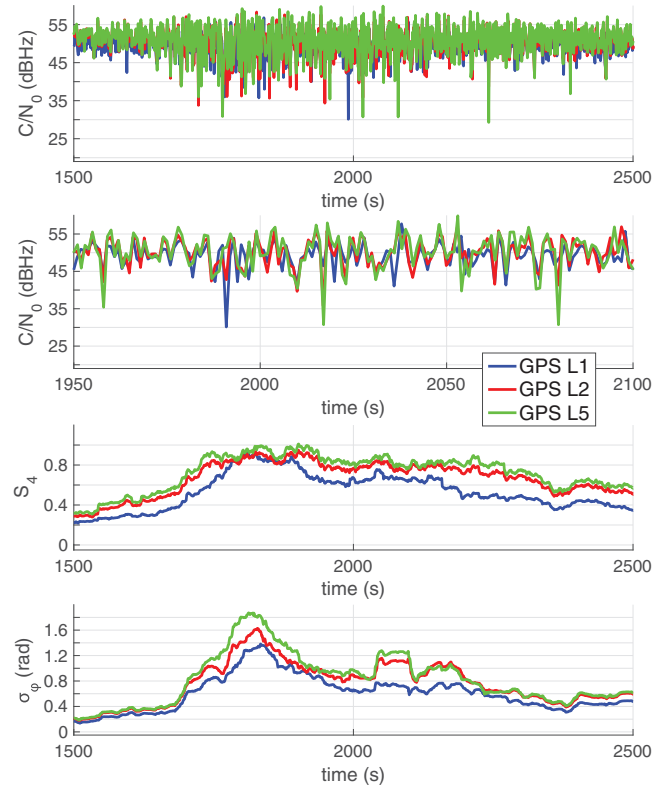


FIGURE 7 Real equatorial ionospheric severe scintillation event recorded over Hanoi, Vietnam, Spring 2015. The two top plots show the C/N_0 for the whole sequence and a zoom to clearly see that deep fades at different frequency bands are uncorrelated [Color figure can be viewed in the online issue, which is available at wileyonlinelibrary.com and www.ion.org]

ture, where the approach originally derived in Vilà-Valls, Closas, and Curran (2017a) is combined with a sequential multivariate AR parameters estimation method (named MF-On-ARKF). This method is compared to:

- i) A third-order fixed bandwidth ($B_w = 15$ Hz) PLL.
- ii) An AKF, adjusting the phase noise variance at the discriminator output from the estimated C/N_0 .
- iii) A single-frequency AR-based KF sequentially estimating the AR parameters (SF-On-ARKF) (Vilà-Valls, Fernández-Prades, Arribas, Curran, & Closas, 2018).
- iv) A single-frequency AR-based KF with off-line fitting to the real scintillation data (SF-Off-ARKF) (Vilà-Valls, Closas, Fernández-Prades, & Curran, 2018).
- v) A multi-frequency AR-based KF with off-line fitting to the real scintillation data (MF-Off-ARKF) (Vilà-Valls, Closas, & Curran, 2017a).

Notice that both SF-Off-ARKF and MF-Off-ARKF are the performance benchmarks for single and multi-frequency processing. We show the characterization of the severe scintillation event under study in Figure 7, where

TABLE 4 RMSE for the LOS phase and scintillation components estimation, considering the equatorial scintillation event shown in Figure 7

	LOS Phase (rad)	Scint Phase (rad)	Scint Amp
PLL	0.4609	-	-
AKF	0.4796	-	-
SF-On-ARKF	0.1668	0.1673	0.03
SF-Off-ARKF	0.0993	0.1076	0.03
MF-On-ARKF	0.1170	0.1233	0.034
MF-Off-ARKF	0.0630	0.0795	0.029

it is clear that there is both amplitude and phase scintillation. From the second zoom plot in Figure 7, we can see that the deep fades at different frequency bands are uncorrelated, a fact that can be exploited using multi-frequency architectures. We consider an initial Doppler $f_{d,0} = 50$ Hz and rate $f_{r,0} = 10$ Hz/s, a nominal $C/N_0 = 40$ dB-Hz, and coherent integration $T_I = 10$ ms. The measure of performance is the RMSE on the carrier phase of interest at L1 and the RMSE for both scintillation components for the methods based on the AR approximation. The RMSE results are given in Table 4. We can see that including the AR scintillation modeling into the state-space formulation, then being able to decouple both phase contributions, drastically improves the mitigation capabilities. Moreover, multi-frequency processing further improves the estimation results. The performance improvement is even more obvious considering L2 and L5 signals, where the scintillation effects are always more severe (Vilà-Valls, Closas, & Curran, 2017a).

7 | CONCLUSIONS AND FUTURE PERSPECTIVES

This section concludes the article, providing further insights and discussing research trends that in our opinion will play an important role in the context of ionospheric scintillation. Throughout this survey, we reviewed the signal-processing landscape in GNSS receivers dealing with ionospheric scintillation, with emphasis on the different detection, monitoring, and mitigation problems and solutions. The main goal being to provide a comprehensive overview of the different methodologies in the literature, together with the discussion on the pros and cons of the different families of methods. To support such discussion, we provided representative examples on the different problems appearing in GNSS: *i*) scintillation detection of both equatorial and high-latitude events; *ii*) low-cost high-latitude scintillation monitoring; and *iii*) adaptive multi-frequency severe equatorial scintillation mitigation. Even

if a plethora of alternatives exist, there are still interesting signal-processing challenges that need to be addressed to boost scientific applications, robustify high-precision carrier-phase-based positioning receivers, and provide reliable solutions for safety-critical applications.

Timely and accurate detection of scintillation events is a relevant task for many categories of receivers. On one side, it allows raising scintillation alerts for high-accuracy applications and critical infrastructures, thus warning users of potential performance degradation. On the other side, precise and unbiased records of scintillations assist the community of physicists working in upper-atmosphere and space weather. Finally, reducing the false alarms, especially those caused by multipath reflections and resembling amplitude scintillation, allows optimization of the use of storage and bandwidth resources in monitoring stations networks. The use of classical amplitude- and phase-scintillation indices is quite common, either relying on visual inspection of time series or on automatic rules based on thresholds, but is limited by the required human effort and capability to reject false alarms, respectively. Machine learning algorithms showed potential, reaching a detection accuracy beyond 98% at the expenses of higher complexity and computational load. Nonetheless, the research is moving toward the design of dedicated receivers and advanced filtering and processing algorithms, which can assure a more correct representation of the dynamics of the atmosphere and, as a consequence, better detection performance.

From a signal-processing perspective, the main challenges in scintillation monitoring go towards *i*) being able to use low-cost and/or mass market receivers; and *ii*) the ability to provide meaningful results in moving platforms. The benefits of deploying a large monitoring network are numerous since it would impact a large variety of applications which rely on GNSS. The main challenges associated to deploying such a dense receiver network being the high cost (and maintenance) of commercial dedicated monitoring receivers and the fact that these receivers require very stable and precise reference oscillators and are typically installed at a known (static) receiver position. While the former directly impacts a rapid deployment, the latter limits their use, for instance, over oceanic regions. An interesting approach using GNSS reflectometry (GNSS-R) has been recently proposed in Camps et al. (2018).

Regarding scintillation mitigation, the main thrusts for further methodological developments are robustness, reliability, accuracy, and precision. Robustness and reliability are in order to ensure a proper receiver behavior in safety-critical applications, such as aviation and autonomous driving. Accuracy and precision are by means of carrier-phase-based positioning techniques. Robust RTK and PPP techniques under scintillation conditions are still

open issues. Some recent attempts are shown in Juan et al. (2018) and Vani et al. (2019). Moreover, efficient scintillation mitigation must be ensured for different types of vehicle dynamics and for using low-cost/mass-market receivers, resulting in additional oscillator-induced phase errors which must be accounted for.

On a more controversial note, the study of ionospheric scintillation and its countermeasures could be potentially relevant in human-induced events such as those recently reported in Zhang et al. (2018). In those experiments, the ionosphere was manipulated through the emission of radio-frequency signals from atmospheric heating facilities, potentially distorting (purposely or not) signals crossing the ionosphere. On another note, high-altitude nuclear explosions/detonations may also impact the ionosphere.

ACKNOWLEDGEMENTS

This work was in part supported by the National Science Foundation under Awards CNS-1815349 and ECCS-1845833, the 2019 TéSA Research Fellowship, and by the DGA/AID under project 2019.65.0068.00.470.75 01.

ORCID

Jordi Vilà-Valls  <https://orcid.org/0000-0001-7858-4171>

Nicola Linty  <https://orcid.org/0000-0001-9795-8693>

Pau Closas  <https://orcid.org/0000-0002-5960-6600>

REFERENCES

- Abadi, P., Saito, S., & Srigutomo, W. (2014). Low-latitude scintillation occurrences around the equatorial anomaly crest over Indonesia. *Annales Geophysicae*, 32(1), 7–17.
- Adewale, A. O., Oyeyemi, E. O., Adeloye, A. B., Mitchell, C. N., Rose, J. A. R., & Cilliers, P. J. (2012). A study of L-band scintillations and total electron content at an equatorial station, Lagos, Nigeria. *Radio Science*, 47(2), 1–12.
- Amin, M. G., Closas, P., Broumandan, A., & Volakis, J. L. (2016). Vulnerabilities, threats, and authentication in satellite-based navigation systems [scanning the issue]. *Proceedings of the IEEE*, 104(6), 1169–1173.
- Anderson, B., & Moore, J. B. (1979). *Optimal filtering*. Englewood Cliffs, NJ: Prentice-Hall.
- Aon, E. F., Othman, A. R., Ho, Y. H., & Shaddad, R. Q. (2015). A study of ionospheric GPS scintillation during solar maximum at UTeM station. *Jurnal Teknologi*, 73, 123–128.
- Aquino, M., Dodson, A., deFranceschi, G., Alfonsi, L., Romano, V., Monico, J.F.G., ... Mitchell, C. (2007). Towards forecasting and mitigating ionospheric scintillation effects on GNSS. *Proceedings of ELMAR* (pp. 63–67), Zadar, Croatia.
- Atilaw, T. Y., Cilliers, P., & Martinez, P. (2017). Azimuth-dependent elevation threshold (adet) masks to reduce multipath errors in ionospheric studies using GNSS. *Advances in Space Research*, 59(11), 2726–2739.
- Axelrad, P., Larson, K., & Jones, B. (2005). Use of the correct satellite repeat period to characterize and reduce site-specific multipath errors. *Proceedings of the International Technical Meeting of the Satellite Division of the Institute of Navigation (ION GPS)* (pp. 2638–2648), Long Beach, CA.
- Banville, S., & Langley, R. B. (2013). Mitigating the impact of ionospheric cycle slips in GNSS observations. *Journal of Geodesy*, 87(2), 179–193.
- Banville, S., Langley, R. B., Saito, S., & Yoshihara, T. (2010). Handling cycle slips in GPS data during ionospheric plasma bubble events. *Radio Science*, 45(6). <https://doi.org/10.1029/2010RS004415>
- Barreau, V., Vigneau, W., Macabiau, C., & Deambrogio, L. (2012). Kalman filter based robust GNSS signal tracking algorithm in presence of ionospheric scintillations. *Proceedings of the 6th ESA Workshop on Satellite Navigation Technologies (NAVITEC) & European Workshop on GNSS Signals and Signal Processing* (pp. 2325–5439), Noordwijk, The Netherlands.
- Beach, T. (1998). *Global positioning system studies of equatorial scintillations* (PhD thesis). Cornell University.
- Beach, T. L., & Kintner, P. M. (2001). Development and use of a GPS ionospheric scintillation monitor. *IEEE Transactions on Geoscience and Remote Sensing*, 39(5), 918–928.
- CALIBRA. Countering GNSS high Accuracy applications Limitation due to ionospheric disturbance in BRAzil. Retrieved from <https://www.gsa.europa.eu/countering-gnss-high-accuracy-applications-limitations-due-ionospheric-disturbances-brazil>.
- Camps, A., Park, H., Juan, J.M., Sanz, J., González-Casado, G., Barbosa, J. ... Orús, R. (2018). Ionospheric scintillation monitoring using GNSS-R? *Proceedings of the IEEE International Geoscience and Remote Sensing Symposium (IGARSS)*, Valencia, Spain.
- Carrano, C. S., Groves, K. M., Mcneil, W. J., & Doherty, P. H. (2012). Scintillation characteristics across the GPS frequency band. *Proceedings of the International Technical Meeting of the Satellite Division of the Institute of Navigation (ION GNSS)* (pp. 1972–1989). Nashville, TN: Nashville Convention Center.
- Carroll, M., Morton, Y. J., & Vinande, E. (2014). Triple frequency GPS signal tracking during strong ionospheric scintillation over Ascension island. *Proceedings of the IEEE/ION Position, Location and Navigation Symposium (PLANS)* (pp. 43–49), San Diego, CA.
- Cesaroni, C., Alfonsi, L., Romero, R., Linty, N., Dovis, F., Veettil, S. V., & Perez, R. O. (2015). Monitoring ionosphere over South America: The MImOSA and MImOSA2 projects. *2015 International Association of Institutes of Navigation World Congress (IAIN)* (pp. 1–7), Prague, Czech Republic.
- Chiou, T.-Y. (2010). *Design of a Doppler-aided GPS navigation system for weak signals caused by strong ionospheric scintillation* (PhD thesis). Stanford University, Department of Aeronautics and Astronautics.
- Chiou, T.-Y., Gebre-Egziaber, D., Walter, T., & Enge, P. (2007). Model analysis on the performance for an inertial aided FLL-assisted PLL carrier tracking loop in the presence of ionospheric scintillation. *Proceedings of the International Technical Meeting of The Institute of Navigation (ITM)*, San Diego, CA.
- Chiou, T.-Y., Seo, J., Walter, T., & Enge, P. (2008). Performance of doppler-aided GPS navigation system for aviation applications under ionospheric scintillation. *Proceedings of the International Technical Meeting of the Satellite Division of the Institute of Navigation (ION GNSS)*, Savannah, GA.
- CIGALA. Concept for Ionospheric-Scintillation Mitigation for Professional GNSS in Latin America. Retrieved from: <http://www.gsa.europa.eu/concept-ionospheric-scintillation-mitigation-professional-gnss-latin-america>.

- Closas, P., Luise, M., Avila-Rodriguez, J., Hegarty, C., & Lee, J. (2017). Advances in signal processing for GNSSs [From the Guest Editors]. *IEEE Signal Processing Magazine*, 34(5), 12–15.
- Coster, A. J., Gaposchkin, E. M., & Thornton, L. E. (1992). Real-time ionospheric monitoring system using GPS. *NAVIGATION*, 39(2), 191–204. <https://doi.org/10.1002/j.2161-4296.1992.tb01874.x>.
- Cristodaro, C., Dovis, F., Linty, N., & Romero, R. (2018). Design of a configurable monitoring station for scintillations by means of a GNSS software radio receiver. *IEEE Geoscience and Remote Sensing Letters*, 15(3), 325–329.
- Curran, J. T., Bavaro, M., & Fortuny-Guasch, J. (2014). An open-loop vector receiver architecture for GNSS-based scintillation monitoring. *Proceedings of the European Navigation Conference (ENC-GNSS)*, Rotterdam, The Netherlands.
- Curran, J. T., Bavaro, M., Fortuny-Guasch, J., & Morrison, A. (2014). Developing an ionospheric scintillation monitoring receiver. *Inside GNSS*, 60–72.
- Curran, J. T., Bavaro, M., Morrison, A., & Fortuny, J. (2015a). Event identification & recording for scintillation monitoring stations. *Proceedings of the International Technical Meeting of the Satellite Division of the Institute of Navigation (ION GNSS+)* (pp. 114–122), Dana Point, CA.
- Curran, J. T., Bavaro, M., Morrison, A., & Fortuny, J. (2015b). Operating a network of multi-frequency software-defined ionosphere monitoring receivers. *Proceedings of the International Technical Meeting of the Satellite Division of the Institute of Navigation (ION GNSS+)*, Tampa, FL.
- Curran, J. T., Bavaro, M., Morrison, A., & Fortuny-Guasch, J. (2014). Developing a multi-frequency GNSS-based scintillation monitoring receiver. *Proceedings of the International Technical Meeting of the Satellite Division of the Institute of Navigation (ION GNSS+)*, Tampa, FL.
- Dardari, D., Closas, P., & Djurić, P. M. (2015). Indoor tracking: Theory, methods, and technologies. *IEEE Transactions on Vehicular Technology*, 64(4), 1263–1278.
- Dardari, D., Falletti, E., & Luise, M. (2011). *Satellite and terrestrial radio positioning techniques: A signal processing perspective*. Cambridge, MA: Academic Press, Elsevier.
- De Oliveira Nascimento Brassarote, G., Souza, E. M., & Monico, G. (2018). s_4 index: Does it only measure ionospheric scintillation? *GPS Solutions*, 22(1), 8.
- Deambrogio, L., & Macabiau, C. (2013). Vector tracking aiding for carrier phase estimation in the presence of ionospheric scintillation. *Proceedings of the International Technical Meeting of the Institute of Navigation (ITM)* (pp. 333–342), San Diego, CA.
- Di Giovanni, G., & Radicella, S. M. (1990). An analytical model of the electron density profile in the ionosphere. *Advances in Space Research*, 10(11), 27–30.
- Doherty, P., Coster, A. J., & Murtagh, W. (2004). Space weather effects of October–November 2003. *GPS Solutions*, 8(4), 267–271.
- Dubei, S., Wahi, R., Mingkhwan, E., & Gwal, A. K. (2005). Study of amplitude and phase scintillation at GPS frequency. *Indian Journal of Radio & Space Physics (IJRSP)*, 34, 402–407.
- Dubey, S., Wahi, R., & Gwal, A. K. (2006). Ionospheric effects on GPS positioning. *Advances in Space Research*, 38(11), 2478–2484.
- Duník, J., Straka, O., Kost, O., & Havlík, J. (2017). Noise covariance matrices in state-space models: A survey and comparison of estimation methods - Part I. *International Journal of Adaptive Control and Signal Processing*, 31(11), 1505–1543.
- Fantinato, S., Rovelli, D., & Crosta, P. (2012). The switching carrier tracking loop under severe ionospheric scintillation. *Proceedings of 6th ESA Workshop on Satellite Navigation Technologies (NAVITEC) & European Workshop on GNSS Signals and Signal Processing*, Noordwijk, The Netherlands.
- Favenza, A., Farasin, A., Linty, N., & Dovis, F. (2017). A machine learning approach to GNSS scintillation detection: Automatic soft inspection of the events. *Proceedings of the International Technical Meeting of the Satellite Division of the Institute of Navigation (ION GNSS+)* (pp. 4103–4111), Portland, OR.
- Fernández-Prades, C., Lo Presti, L., & Falletti, E. (2011). Satellite radiolocalization from GPS to GNSS and beyond: Novel technologies and applications for civil mass market. *Proceedings of the IEEE*, 99(11), 1882–1904.
- Flach, P. (2012). *Machine learning: The art and science of algorithms that make sense of data*. Cambridge, UK: Cambridge University Press.
- Fohlmeister, F., Antreich, F., & Nossek, J. A. (2018). Dual Kalman filtering based GNSS phase tracking for scintillation mitigation. *Proceedings of the IEEE/ION Position, Location and Navigation Symposium (PLANS)*, Monterey, CA.
- Forte, B. (2005). Optimum detrending of raw GPS data for scintillation measurements at auroral latitudes. *Journal of Atmospheric and Solar-Terrestrial Physics*, 67(12), 1100–1109.
- Fortunato, M., Ravanelli, M., & Mazzoni, A. (2019). Real-time geophysical applications with Android GNSS raw measurements. *Remote Sensing*, 11(18), 2113.
- Franzese, G., Linty, N., & Dovis, F. (2020). Semi-supervised GNSS scintillations detection based on DeepInfomax. *Applied Sciences*, 10(1), 381.
- Fu, W., Han, S., Rizos, C., Knight, M., & Finn, A. (1999). Real-time ionospheric scintillation monitoring. *Proceedings of the International Technical Meeting of the Satellite Division of the Institute of Navigation (ION GPS)* (pp. 14–17), Nashville, TN.
- Fujiwara, T., & Tsujii, T. (2016). GBAS availability assessment and modeling of ionospheric scintillation effects. *NAVIGATION*, 63(4), 405–413. <https://doi.org/10.1002/navi.160>.
- Ghafoori, F. (2012). *Modeling the impact of equatorial ionospheric irregularities on GPS receiver performance* (PhD thesis). Department of Geomatics Engineering, The University of Calgary.
- Giger, K., Henkel, P., & Günther, C. (2009). Multi-frequency, multi-satellite carrier tracking. *Proceedings of the 4th European Workshop on GNSS Signals and Signal Processing*, Oberpfaffenhofen, Germany.
- Goncharenko, L. P., Coster, A. J., Chau, J. L., & Valladares, C. E. (2010). Impact of sudden stratospheric warmings on equatorial ionization anomaly. *Journal of Geophysical Research: Space Physics*, 115(A10). <https://doi.org/10.1029/2010JA015400>
- Goncharenko, L. P., Chau, J. L., Liu, H.-L., & Coster, A. J. (2010). Unexpected connections between the stratosphere and ionosphere. *Geophysical Research Letters*, 37(10). <https://doi.org/10.1029/2010GL043125>
- GPStation-6 Triple-Frequency GISTM Receiver. Retrieved from <https://novatel.com/support/previous-generation-products-drop-down/previous-generation-products/gpstation-6-receiver>.
- Henkel, P., Giger, K., & Gunther, C. (2009). Multifrequency, multi-satellite vector phase-locked loop for robust carrier tracking. *IEEE Journal of Selected Topics in Signal Processing*, 3(4), 674–681.

- Humphreys, T. E., Psiaki, M. L., Hinks, J. C., O'Hanlon, B., & Kintner, P. M. (2009). Simulating ionosphere-induced scintillation for testing GPS receiver phase tracking loops. *IEEE Journal of Selected Topics in Signal Processing*, 3(4), 707–715.
- Humphreys, T. E., Psiaki, M. L., & Kintner, P. M. (2005). GPS carrier tracking loop performance in the presence of ionospheric scintillations. *Proceedings of the International Technical Meeting of the Satellite Division of The Institute of Navigation (ION GNSS)* (pp. 156–167), Long Beach, CA.
- Humphreys, T. E., Psiaki, M. L., & Kintner, P. M. (2010). Modeling the effects of ionospheric scintillation on GPS carrier phase tracking. *IEEE Transactions on Aerospace and Electronic Systems*, 46(4), 1624–1637.
- International Telecommunication Union. (2013). Ionospheric propagation data and prediction methods required for the design of satellite services and systems. Recommendation ITU-R p.531-12, Tech. Rep., International Telecommunication Union (ITU).
- Jacobsen, K. S., & Dähnn, M. (2014). Statistics of ionospheric disturbances and their correlation with GNSS positioning errors at high latitudes. *Journal of Space Weather and Space Climate*, 4(A27). <https://doi.org/10.1051/swsc/2014024>
- Jakowski, N., Béniguel, Y., De Franceschi, G., Hernández Pajares, M., Jacobsen, K. S., Stanislawski, I., & Wautelet, G. (2012). Monitoring, tracking and forecasting ionospheric perturbations using GNSS techniques. *Journal of Space Weather and Space Climate*, 2(A22). <https://doi.org/10.1051/swsc/2012022>
- Jiao, Y., Hall, J. J., & Morton, Y. T. (2017a). Automatic equatorial GPS amplitude scintillation detection using a machine learning algorithm. *IEEE Transactions on Aerospace and Electronic Systems*, 53(1), 405–418.
- Jiao, Y., Hall, J. J., & Morton, Y. T. (2017b). Automatic GPS phase scintillation detector using a machine learning algorithm. *Proceedings of the International Technical Meeting of The Institute of Navigation (ITM)* (pp. 1160–1172), Monterey, CA.
- Jiao, Y., Hall, J. J., & Morton, Y. T. (2016). Performance evaluations of an equatorial GPS amplitude scintillation detector using a machine learning algorithm. *Proceedings of the International Technical Meeting of the Satellite Division of The Institute of Navigation (ION GNSS+)* (pp. 195–199), Portland, OR.
- Jiao, Y., Hall, J. J., & Morton, Y. T. (2017c). Performance evaluation of an automatic GPS ionospheric phase scintillation detector using a machine-learning algorithm. *NAVIGATION*, 64(3), 391–402. <https://doi.org/10.1002/navi.188>.
- Jiao, Y., & Morton, Y. T. (2015). Comparison of the effect of high-latitude and equatorial ionospheric scintillation on GPS signals during the maximum of solar cycle 24. *Radio Science*, 50(9) 886–903.
- Jiao, Y., Morton, Y. T., Taylor, S., & Pelgrum, W. (2013a). Characterization of high-latitude ionospheric scintillation of GPS signals. *Radio Science*, 48(6), 698–708.
- Jiao, Y., Morton, Y., Taylor, S., & Pelgrum, W. (2013b). High latitude ionosphere scintillation characterization. *Proceedings of the International Technical Meeting of The Institute of Navigation (ITM)* (pp. 579–584), San Diego, CA.
- Jiao, Y., Rino, C., & Morton, Y. T. (2018). Ionospheric scintillation simulation on equatorial GPS signals for dynamic platforms. *NAVIGATION*, 65(2), 263–274. <https://doi.org/10.1002/navi.231>.
- Jiao, Y., Xu, D., Morton, Y., & Rino, C. (2016). Equatorial scintillation amplitude fading characteristics across the GPS frequency bands. *NAVIGATION*, 63(3), 267–281. <https://doi.org/10.1002/navi.146>.
- Jiao, Y., Xu, D., Rino, C. L., Morton, Y. T., & Carrano, C. S. (2018). A multi-frequency GPS signal strong equatorial ionospheric scintillation simulator: Algorithm, performance, and characterization. *IEEE Transactions on Aerospace and Electronic Systems*, 54(4), 1947–1965.
- Juan, J. M., González-Casado, G., Rovira-Garcia, A., Camps, A., Riba, J., Barbosa, J., & Orus, R. (2018). Feasibility of precise navigation in high and low latitude regions under scintillation conditions. *Journal of Space Weather and Space Climate*, 8(A05). <https://doi.org/10.1051/swsc/2017047>
- Kaplan, E. D. (Ed.) (2006). *Understanding GPS: Principles and applications* (2nd ed.). Norwood, MA: Artech House.
- Kassabian, N., & Morton, Y. J. (2014). Extending integration time for Galileo tracking robustness under ionosphere scintillation. *Proceedings of the IEEE/ION Position, Location and Navigation Symposium (PLANS)* (pp. 59–72), Monterey, CA.
- Kintner, P. M., Humphreys, T. E., & Hinks, J. (2009). GNSS and ionospheric scintillation. How to survive the next solar maximum. *Inside GNSS*, 22–33.
- Lachapelle, G., & Broumandan, A. (2016). Benefits of GNSS IF data recording. *Proceedings of the European Navigation Conference (ENC)*, Helsinki, Finland.
- LaMountain, G., Vilà-Valls, J., & Closas, P. (2018). Bayesian covariance estimation for Kalman filter based digital carrier synchronization. *Proceedings of the International Technical Meeting of the Satellite Division of the Institute of Navigation (ION GNSS+)*, Miami, FL.
- Lashley, M., Bevilacqua, D. M., & Hung, J. Y. (2009). Performance analysis of vector tracking algorithms for weak GPS signals in high dynamics. *IEEE Journal of Selected Topics in Signal Processing*, 3(4), 661–673.
- Lee, J., Morton, J., Lee, J., Moon, H., & Seo, J. (2017). Monitoring and mitigation of ionospheric anomalies for GNSS-based safety critical systems: A review of up-to-date signal processing techniques. *IEEE Signal Processing Magazine*, 34(5) 96–110.
- Lin, T., Lachapelle, G., & Souto Fortes, L. P. (2014). How do modern GNSS signal processing techniques deal with equatorial ionospheric scintillation. *Inside GNSS*, 26–34.
- Linty, N., & Dovič, F. (2019). An open-loop receiver architecture for monitoring of ionospheric scintillations by means of GNSS signals. *Applied Sciences*, 9(12), 2482.
- Linty, N., Dovič, F., & Alfonsi, L. (2018). Software-defined radio technology for gnss scintillation analysis: bring antarctica to the lab. *GPS Solutions*, 22(4), 96.
- Linty, N., Farasin, A., Favenza, A., & Dovič, F. (2019). Detection of GNSS ionospheric scintillations based on machine learning decision tree. *IEEE Transactions on Aerospace and Electronic Systems*, 55(1), 303–317.
- Linty, N., Minetto, A., Dovič, F., & Spogli, L. (2018). Effects of phase scintillation on the GNSS positioning error during the September 2017 storm at Svalbard. *Space Weather*, 16(9), 1317–1329.
- Linty, N., Romero, R., Dovič, F., & Alfonsi, L. (2015). Benefits of GNSS software receivers for ionospheric monitoring at high latitudes. *Proceedings of the 1st URSI Atlantic Radio Science Conference (URSI AT-RASC)* (pp. 1–6). Las Palmas, Spain: IEEE.

- López-Salcedo, J., Peral-Rosado, J., & Seco-Granados, G. (2014). Survey on robust carrier tracking techniques. *IEEE Communications Surveys & Tutorials*, 16(2), 670–688.
- Macabiau, C., Deambrogio, L., Barreau, V., Vigneau, W., Valette, J.-J., Artaud, G., ... Ries, L. (2012). Kalman filter based robust GNSS signal tracking algorithm in presence of ionospheric scintillations. *Proceedings of the International Technical Meeting of the Satellite Division of the Institute of Navigation (ION GNSS)* (pp. 3420–3434), Nashville, TN.
- Mao, X., Morton, Y. T., Zhang, L., & Kou, Y. (2010). GPS carrier signal parameters estimation under ionospheric scintillation. *Proceedings of the International Technical Meeting of the Satellite Division of the Institute of Navigation (ION GNSS)*, Portland, OR.
- Marçal, J., & Nunes, F. (2016). Robust vector tracking for GNSS carrier phase signals. *Proceedings of the 2016 International Conference on Localization and GNSS (ICL-GNSS)*, Barcelona, Spain.
- Marçal, J., Nunes, F., & Sousa, F. (2016). Performance of a scintillation robust vector tracking for GNSS carrier phase signals. *Proceedings of the 8th ESA Workshop on Satellite Navigation Technologies and European Workshop on GNSS Signals and Signal Processing (NAVITEC)*, Noordwijk, The Netherlands.
- Marçal, J., Nunes, F., & Sousa, F. (2017). Robust vector tracking loop for carrier phase signals with separate estimation of common and single channel errors. *Proceedings of the International Technical Meeting of The Institute of Navigation (ITM)*, Monterey, CA.
- Middlestead, R. W. (2017). *Digital communications with emphasis on data modems: Theory, analysis, design, simulation, testing, and applications*. Hoboken, NJ: John Wiley & Sons.
- Miriyala, S., Koppireddi, P. R., & Chanamallu, S. R. (2015). Robust detection of ionospheric scintillations using MF-DFA technique. *Earth, Planets and Space*, 67(98). <https://doi.org/10.1186/s40623-015-0268-1>
- Mushini, S. C., Jayachandran, P. T., Langley, R. B., MacDougall, J. W., & Pokhotelov, D. (2012). Improved amplitude-and phase-scintillation indices derived from wavelet detrended high-latitude GPS data. *GPS Solutions*, 16(3), 363–373.
- Myer, G., Morton, Y., & Schipper, B. (2017). Ionospheric scintillation effects on GPS pseudorange and carrier phase measurements and an adaptive algorithm to limit position errors during scintillation. *Proceedings of the International Technical Meeting of The Institute of Navigation (ITM)*, Monterey, CA.
- Najmafshar, M., Ghafoori, F., & Skone, S. (2013). Robust receiver design for equatorial regions during solar maximum. *Proceedings of the International Technical Meeting of the Satellite Division of the Institute of Navigation (ION GNSS+)*, Nashville, TN.
- Ouassou, M., Kristiansen, O., Gjevestad, J. G. O., Jacobsen, K. S., & Andalsvik, Y. L. (2016). Estimation of scintillation indices: A novel approach based on local kernel regression methods. *International Journal of Navigation and Observation*, 2016.
- Pelgrum, W., Morton, Y., van Graas, F., Gunawardena, S., Bakich, M., Charney, D., & Vikram, P. (2011). Measurement and analysis of artificially-generated and natural ionosphere scintillations effects on GNSS signals. *Proceedings of the International Technical Meeting of The Institute of Navigation (ITM)*, San Diego, CA (pp. 950–958).
- Peng, S. (2012). *A multi-constellation multi-frequency GNSS software receiver design for ionosphere scintillation studies* (PhD thesis). Virginia Polytechnic Institute and State University.
- Piersanti, M., Materassi, M., Cicone, A., Spogli, L., Zhou, H., & Ezquer, R. G. (2018). Adaptive local iterative filtering: A promising technique for the analysis of nonstationary signals. *Journal of Geophysical Research: Space Physics*, 123(1) 1031–1046.
- PolaRxS. Retrieved from <https://www.septentrio.com/en/products/gnss-receivers/reference-receivers/polarx5s>.
- Prieto Cerdeira, R., & Béniguel, Y. (2011). The MONITOR project: Architecture, data and products. *Proceedings of Ionospheric Effects Symposium*, Alexandria, VA.
- Prikryl, P., Jayachandran, P. T., Mushini, S. C., & Richardson, I. G. (2014). High-latitude GPS phase scintillation and cycle slips during high-speed solar wind streams and interplanetary coronal mass ejections: A superposed epoch analysis. *Earth, Planets and Space*, 66(1).
- Psiaki, M. L., Humphreys, T. E., Cerruti, A., Powell, S., & Kintner, P. M. (2007). Tracking L1 C/A and L2C signals through ionospheric scintillations. *Proceedings of the International Technical Meeting of the Satellite Division of the Institute of Navigation (ION GNSS)*, Fort Worth, TX.
- Pullen, S., Park, Y. S., & Enge, P. (2009). Impact and mitigation of ionospheric anomalies on ground-based augmentation of GNSS. *Radio Science*, 44(1). <https://doi.org/10.1029/2008RS004084>
- Qin, W., & Dervis, F. (2018). Effects of interference mitigation methods on scintillation detection. *Proceedings of the 9th ESA Workshop on Satellite Navigation Technologies and European Workshop on GNSS Signals and Signal Processing (NAVITEC)* (pp. 1–8). Noordwijk, The Netherlands: IEEE.
- Rezende, L. F. C., de Paula, E. R., Stephany, S., Kantor, I. J., Muella, M. T. A. H., de Siqueira, P. M., & Correa, K. S. (2010). Survey and prediction of the ionospheric scintillation using data mining techniques. *Space Weather*, 8(6). <https://doi.org/10.1029/2009SW000532>
- Rino, C., Breitsch, B., Morton, Y., Jiao, Y., Xu, D., & Carrano, C. (2018). A compact multi-frequency GNSS scintillation model. *NAVIGATION*, 65(4), 563–569. <https://doi.org/10.1002/navi.263>.
- Romero, R., & Dervis, F. (2014). Towards analyzing the effect of interference monitoring in GNSS scintillation. In R. Notarpietro, F. Dervis, G. De Franceschi, & M. Aquino (Eds.), *Mitigation of ionospheric threats to GNSS: An appraisal of the scientific and technological outputs of the TRANSMIT project*. Rijeka, Croatia: IntechOpen.
- Romero, R., Linty, N., Dervis, F., & Field, R. V. (2016). A novel approach to ionospheric scintillation detection based on an open loop architecture. *Proceedings of the 8th ESA Workshop on Satellite Navigation Technologies and European Workshop on GNSS Signals and Signal Processing (NAVITEC)*, Noordwijk, The Netherlands.
- Romero Gaviria, R. M. (2015). *Estimation techniques and mitigation tools for ionospheric effects on GNSS receivers* (PhD thesis). Politecnico di Torino.
- Secan, J. A., Bussey, R. M., & Fremouw, E. J. (1997). High-latitude upgrade to the wideband ionospheric scintillation. *Radio Science*, 32(4), 1567–1574.
- Seco-Granados, G., Lopez-Salcedo, J. A., Jiménez-Baños, D., & López-Risueño, G. (2012). Challenges in indoor global navigation satellite systems: Unveiling its core features in signal processing. *IEEE Signal Processing Magazine*, 29(2), 108–131.
- Seo, J. (2010). *Overcoming ionospheric scintillation for worldwide GPS aviation* (PhD thesis). Stanford University, Department of Aeronautics and Astronautics.

- Seo, J., & Walter, T. (2014). Future dual-frequency GPS navigation system for intelligent air transportation under strong ionospheric scintillation. *IEEE Transactions on Intelligent Transportation Systems*, 15(5), 2224–2236.
- Skone, G., Lachapelle, G., Yao, D., Yu, W., & Watson, R. (2005). Investigating the impact of ionospheric scintillation using a GPS software receiver. *Proceedings of the International Technical Meeting of the Satellite Division of the Institute of Navigation (ION GNSS)*, Long Beach, CA.
- Sokolova, N., Morrison, A., & Curran, J. T. (2015). High latitude phase scintillation decorrelation across GNSS frequencies — Exploring the impact of scintillation on multi-frequency users. *European Journal of Navigation*, 13(3), 45–51.
- Sousa, F., & Nunes, F. (2014a). Performance analysis of a VDFLL GNSS receiver architecture under ionospheric scintillation and multipath conditions. *Proceedings of the IEEE/ION Position, Location, and Navigation Symposium (PLANS)*, Monterey, CA.
- Sousa, F., & Nunes, F. (2014b). Performance comparison of a VDFLL versus VDLL and scalar GNSS receiver architectures in harsh scenarios. *Proceedings of the 7th ESA Workshop on Satellite Navigation Technologies and European Workshop on GNSS Signals and Signal Processing (NAVITEC)*, Noordwijk, The Netherlands.
- Spilker, J. J. (1996). Fundamentals of signal tracking theory. In B. W. Parkinson & J. J. Spilker (Eds.), *Global positioning system: Theory and applications* (Vol. I, pp. 245–328), American Institute of Aeronautics and Astronautics.
- Spogli, L., Romano, V., De Franceschi, G., Alfonsi, L., Plakidis, E., Cesaroni, C., & Vani, B. (2014). A filtering method developed to improve gnss receiver data quality in the CALIBRA project. In R. Notarpietro, F. Dosis, G. De Franceschi, & M. Aquino (Eds.), *Mitigation of Ionospheric Threats to GNSS: An Appraisal of the Scientific and Technological Outputs of the TRANSMIT Project*, Rijeka, Croatia: IntechOpen.
- Strangeways, H. J., & Tiwari, R. (2013). Prediction and mitigation of ionospheric scintillation and tracking jitter for GNSS positioning. In *Proc. ELMAR* (pp. 319–322), Zadar, Croatia.
- Susi, M., Andreotti, M., & Aquino, M. (2014). Kalman filter based PLL robust against ionospheric scintillation. In R. Notarpietro, F. Dosis, G. De Franceschi, & M. Aquino (Eds.), *Mitigation of ionospheric threats to GNSS: An appraisal of the scientific and technological outputs of the TRANSMIT project* (pp. 23–36). Rijeka, Croatia: IntechOpen.
- Susi, M., Aquino, M., Romero, R., Dosis, F., & Andreotti, M. (2014). Design of a robust receiver architecture for scintillation monitoring. *Proceedings of the IEEE/ION Position, Location and Navigation Symposium (PLANS)* (pp. 73–81), Monterey, CA.
- Taylor, S., Morton, Y., Jiao, Y., Triplett, J., & Pelgrum, W. (2012). An improved ionosphere scintillation event detection and automatic trigger for GNSS data collection systems. *Proceedings of the International Technical Meeting of The Institute of Navigation (ITM)* (pp. 1563–1569), Newport Beach, CA.
- Tiwari, R., Skone, S., Tiwari, S., & Strangeways, H. J. (2011). WMod assisted PLL GPS software receiver for mitigating scintillation affect in high latitude region. *Proceedings of the 23th URSI General Assembly and Scientific Symposium*, Istanbul, Turkey.
- TRANSMIT. Training Research and Applications Network to Support the Mitigation of Ionospheric Threats. Retrieved from: <https://cordis.europa.eu/project/id/264476>.
- Van Dierendonck, A. J. (2009). GPS ionospheric scintillation & TEC monitor. Technical Report, Navigation Science and Technology for Africa, ICTP Seminar. User's Manual.
- Van Dierendonck, A. J., Klobuchar, J., & Hua, Q. (1993). Ionospheric scintillation monitoring using commercial single frequency C/A code receivers. *Proceedings of the International Technical Meeting of the Satellite Division of the Institute of Navigation (ION GPS)* (pp. 1333–1342), Salt Lake City, UT.
- Vani, B. C., Forte, B., Monico, J. F. G., Skone, S., Shimabukuro, M. H., de O. Moraes, A., & Marques, H. A. (2019). A novel approach to improve GNSS Precise Point Positioning during strong ionospheric scintillation: Theory and demonstration. *IEEE Transactions on Vehicular Technology*, 68(5), 4391–4403.
- Vikram, P., Morton, Y. T., & Pelgrum, W. (2011). Event driven GPS data collection system for studying ionospheric scintillation. *Proceedings of the International Technical Meeting of the Satellite Division of the Institute of Navigation (ION GNSS)* (pp. 3903–3909), Portland, OR.
- Vilà-Valls, J., Closas, P., & Curran, J. T. (2017a). Multi-frequency GNSS robust carrier tracking for ionospheric scintillation mitigation. *Journal of Space Weather and Space Climate*, 7(A26). <https://doi.org/10.1051/swsc/2017020>
- Vilà-Valls, J., Closas, P., & Curran, J. T. (2017). Performance analysis of multi-frequency GNSS carrier tracking for strong ionospheric scintillation mitigation. *Proceedings of the 25th European Signal Processing Conference (EUSIPCO)*, Kos Island, Greece.
- Vilà-Valls, J., Closas, P., & Fernández-Prades, C. (2015a). Advanced KF-based methods for GNSS carrier tracking and ionospheric scintillation mitigation. *Proceedings of the IEEE Aerospace Conference*, Big Sky, MT.
- Vilà-Valls, J., Closas, P., & Fernández-Prades, C. (2015b). On the identifiability of noise statistics and adaptive KF design for robust GNSS carrier tracking. *Proceedings of the IEEE Aerospace Conference*, Big Sky, MT.
- Vilà-Valls, J., Closas, P., Fernández-Prades, C., & Curran, J. T. (2018). On the mitigation of ionospheric scintillation in advanced GNSS receivers. *IEEE Transactions on Aerospace and Electronic Systems*, 54(4), 1692–1708.
- Vilà-Valls, J., Closas, P., Fernández-Prades, C., López-Salcedo, J. A., & Seco-Granados, G. (2015). Adaptive GNSS carrier tracking under ionospheric scintillation: Estimation vs mitigation. *IEEE Communications Letters*, 19(6), 961–964.
- Vilà-Valls, J., Closas, P., Navarro, M., & Fernández-Prades, C. (2017). Are PLLs dead? A tutorial on Kalman filter-based techniques for digital carrier synchronization. *IEEE Aerospace and Electronic Systems Magazine*, 32(7), 28–45.
- Vilà-Valls, J., López-Salcedo, J. A., & Seco-Granados, G. (2013). An interactive multiple model approach for robust GNSS carrier phase tracking under scintillation conditions. *Proceedings IEEE International Conference on Acoustics, Speech and Signal Processing (ICASSP)*, Vancouver, Canada.
- Vilà-Valls, J., Fernández-Prades, C., Curran, J. T., & Closas, P. (2017). Challenges of using low-cost GNSS receivers for ionospheric scintillation monitoring. *Proceedings of the 6th ESA International Colloquium on Scientific and Fundamental Aspects of GNSS/Galileo*, Valencia, Spain.
- Vilà-Valls, J., Fernández-Prades, C., Closas, P., & Arribas, J. (2017b). Noise statistics estimation techniques for robust GNSS carrier tracking. *Proceedings of the International Technical Meeting of the*

- Satellite Division of the Institute of Navigation (ION GNSS+)*, Portland, OR.
- Vilà-Valls, J., Fernández-Prades, C., Arribas, J., Curran, J. T., & Closas, P. (2018). On-line model learning for adaptive GNSS ionospheric scintillation estimation and mitigation. *Proceedings of the IEEE/ION Position, Location and Navigation Symposium (PLANS)*, Monterey, CA.
- Warnant, R., Urlich, F., Aquino, M., Bidaine, B., Gherm, V., Hoque, M., & Jakowski, N. (2009). Mitigation of ionospheric effects on GNSS. *Annals of Geophysics*, 52(3), 373–390.
- Warren, D. L. M., & Raquet, J. F. (2003). Broadcast vs. precise gps ephemerides: A historical perspective. *GPS Solutions*, 7(3), 151–156.
- Won, J. H. (2014). A novel adaptive digital phase-lock-loop for modern digital GNSS receivers. *IEEE Communications Letters*, 18(1), 46–49.
- Won, J.-H., Eissfeller, B., Pany, T., & Winkel, J. (2012). Advanced signal processing scheme for GNSS receivers under ionospheric scintillation. *Proceedings of the IEEE/ION Position, Location and Navigation Symposium (PLANS)* (pp. 44–49), Myrtle Beach, SC.
- Xu, D., & Morton, Y. (2018). A semi-open loop GNSS carrier tracking algorithm for monitoring strong equatorial scintillation. *IEEE Transactions on Aerospace and Electronic Systems*, 54(2), 772–738.
- Xu, D., & Morton, Y. (2015). GPS carrier parameters characterization during strong equatorial ionospheric scintillation. *Proceedings of the International Technical Meeting of The Institute of Navigation (ITM)*, Dana Point, CA.
- Xu, D., Morton, Y., Akos, D., & Walter, T. (2015a). GPS multi-frequency carrier phase characterization during strong equatorial ionospheric scintillation. *Proceedings of the International Technical Meeting of the Satellite Division of the Institute of Navigation (ION GNSS+)* (pp. 3787–3796), Tampa, FL.
- Xu, D., Morton, Y., Akos, D., & Walter, T. (2015b). GPS multi-frequency carrier phase characterization during strong equatorial ionospheric scintillation. *Proceedings of the International Technical Meeting of the Satellite Division of The Institute of Navigation (ION GNSS+)*, Tampa, FL.
- Xu, D., Morton, Y. T., Jiao, Y., & Rino, C. (2017). Robust GPS carrier tracking algorithms during strong equatorial scintillation for dynamic platforms. *Proceedings of the International Technical Meeting of the Satellite Division of the Institute of Navigation (ION GNSS+)*, Portland, OR.
- Xu, D., Jade Morton, Y., Jiao, Y., Rino, C., & Yang, R. (2018). Implementation and performance evaluation of a vector-based receiver during strong equatorial scintillation on dynamic platforms. *Proceedings of the International Technical Meeting of the Satellite Division of the Institute of Navigation (ION GNSS+)*, Miami, FL.
- Yin, H., Morton, Y., & Carroll, M. (2014). Implementation and performance analysis of a multi-frequency GPS signal tracking algorithm. *Proceedings of the International Technical Meeting of the Satellite Division of the Institute of Navigation (ION GNSS+)*, Tampa, FL.
- Yoon, M., Kim, D., Pullen, S., & Lee, J. (2019). Assessment and mitigation of equatorial plasma bubble impacts on category I GBAS operations in the Brazilian region. *NAVIGATION*, 66(3), 643–659. <https://doi.org/10.1002/navi.328>.
- Yu, W., Lachapelle, G., & Skone, S. (2006). PLL performance for signals in the presence of thermal noise, phase noise, and ionospheric scintillation. *Proceedings of the International Technical Meeting of the Satellite Division of the Institute of Navigation (ION GNSS)*, Fort Worth, TX.
- Zhang, X., Frolov, V., Zhao, S., Zhou, C., Wang, Y., Ryabov, A., & Zhai, D. (2018) The first joint experimental results between SURA and CSES. *Earth and Planetary Physics*, 2(6), 527–537.
- Zhang, L., & Morton, Y. T. (2009). Tracking GPS signals under ionosphere scintillation conditions. *Proceedings of the International Technical Meeting of the Satellite Division of the Institute of Navigation (ION GNSS)* (pp. 227–234), Savannah, GA.
- Zhang, L., Morton, Y. T., & Miller, M. M. (2010). A variable gain adaptive Kalman filter-based GPS carrier tracking algorithms for ionosphere scintillation signals. *Proceedings of the International Technical Meeting of The Institute of Navigation (ITM)* (pp. 3107–3114), San Diego, CA.
- Zhang, L., Morton, Y. T., Van Graas, F., & Beach, T. (2010). Characterization of GNSS signal parameters under ionosphere scintillation conditions using software-based tracking algorithms. *Proceedings of the IEEE/ION Position, Location and Navigation Symposium (PLANS)* (pp. 264–275), Indian Wells, CA.

How to cite this article: Vilà-Valls J, Linty N, Closas P, Dovis F, Curran JT. Survey on signal processing for GNSS under ionospheric scintillation: Detection, monitoring, and mitigation. *NAVIGATION*. 2020; 1–24. <https://doi.org/10.1002/navi.379>